



Rheinische Friedrich-Wilhelms-Universität Bonn

Geographisches Institut

**Comparison of viticultural management practices
in Rheinhessen using UAV-based multispectral
remote sensing data**

Bachelorarbeit Geographie (B.Sc.)

vorgelegt von: Noah Greupner

Abgabe: Bonn, Mai 2022

Table of Contents

List of figures	ii
List of tables.....	iii
1. Introduction.....	1
2. Materials and methods	6
2.1 Study area.....	6
2.1.1 Model vineyards.....	7
2.1.2 Experimental design.....	10
2.2 Field equipment.....	12
2.2.1 Ground Control Points	12
2.2.2 UAV	13
2.2.3 Multispectral camera.....	13
2.3 Flight Planning	14
2.4 Image acquisition	15
2.5 Image processing.....	16
2.6 Statistical analysis	17
3. Results.....	19
3.1 Aerial imagery.....	19
3.2 Spatiotemporal management effects	22
4. Discussion	27
4.1 Image evaluation	27
4.2 NDVI evaluation	28
4.3 Spatiotemporal management effects	29
5. Conclusion and outlook	31
6. Bibliography.....	33
7. Appendices.....	38

List of figures

Figure 1: Location of the three investigated model vineyards (A1-A3).....	6
Figure 2: Overview of the three model vineyards	9
Figure 3: Experimental design of A1	10
Figure 4: Ground Control Point on a model vineyard	12
Figure 5: The Parrot Sequoia multispectral camera and sunshine sensor and the DJI Mavic 2 Pro with the attached Parrot Sequoia	14
Figure 6: Screenshot of the Pix4DCapture application during the planning of a flight	14
Figure 7: Example of the processed RGB and multispectral imagery.....	19
Figure 8: NDVI images of the three model vineyards for each of the individual flights ...	21
Figure 9: Histograms and cumulative frequencies of NDVI values before and after inter-row management	22
Figure 10: Boxplots of NDVI values as a function of time and management regime.....	26

List of tables

Table 1: Information about the different model vineyards	11
Table 2: Wavelengths of the different Parrot Sequoia bands.	13
Table 3: Detailed information about the individual flights.....	15
Table 4: Ground Sampling Distance of the RGB and multispectral orthophotos.....	20
Table 5: Descriptive statistics of the NDVI analysis of the model vineyards before and after the inter-row management.	23

1. Introduction

Grapevine is one of the oldest cultivated plants in human history and it is grown in many parts of the world. In total, seven million hectares worldwide are occupied by vineyards (PAIOLA et al. 2020). A few thousand years ago, viticulture was largely confined to the Mediterranean and European regions. In recent centuries, however, new areas of cultivation have been added around the world. Today, wine is also grown in North and South America, Australia, South Africa, and Asia. Considering this, vineyards influence the environment and, thus, have a huge impact on ecosystem services (ES) on a global level.

In Germany, grapevine is cultivated on over 100.000 hectares (DEUTSCHES WEININSTITUT 2022). Traditionally, German viticultural landscapes consisted of xerothermic slopes with transverse terraces and dry stone walls that created heterogeneous and species-rich agroecosystems with high conservation value (PAIOLA et al. 2020). In addition, viticulture and orcharding were often practised in the same area in dual-use. Because of these factors, German vineyards host rare flora and fauna specialized to the microclimatic conditions. For example, many plants from the Mediterranean region grow here (GEMMICH 2017). Furthermore, vineyards are home to rare species such as snakes, lizards, butterflies, and crickets (HOFMANN 2014).

However, modern viticulture, also in Germany, has turned these heterostructural habitats of high biodiversity into species-poor monocultures. Among other factors, soil tillage operations, herbicide applications, and intensive fertilization have led vineyards to be among the most intensively managed agroecosystems worldwide (KATAYAMA et al. 2019). In addition, the German land clearings from 1960 to 1990, which were mostly a consequence of poor economic situations, contributed to forming monocultural landscapes (GEMMICH 2017). The clearings resulted in increased field sizes and reduced presence of semi-natural areas that are of high ecological value for the ecosystem and that are a precondition for the occurrence of many species in vineyard-dominated landscapes. On top of that, viticulture reacts comparatively sensitive to the ongoing climate change (HANNAH et al. 2013). In this context, extreme weather events like heatwaves, dryness, hail, or floodings are increasing in frequency (IPCC 2018), already posing major challenges for winegrowers, like increased erosion, water stress, or late frost events (FRAGA et al. 2012).

All these processes threaten ES and biodiversity in vineyards at the field and landscape level (PUIG-MONTSERRAT et al. 2017; ZANETTIN et al. 2021). HALL et al. (2020), for example,

show that viticultural management intensification reduces plant species richness and, therefore, declines ecosystem stability and resilience. In this context, it must also be said that biodiversity decline, which is a consequence of agricultural intensification, is one of the greatest threats to global food security and humanity in general (EUROPEAN COMMISSION 2021; MOLOTOKS et al. 2017).

However, as already described above, vineyards have a huge potential for biodiversity conservation and delivery of biodiversity-mediated ES that is currently not being fully exploited (PAIOLA et al. 2020). Thus, agroecological studies about ES and biodiversity patterns in viticulture have increased in the last years, often dealing with different management effects on ES and biodiversity (cf. GUERRA u. STEENWERTH 2012; KATAYAMA et al. 2020). Moreover, new alternative management strategies, such as sheep grazing, are investigated to increase climate adaptation and biodiversity and thus improve ES in vineyards (cf. LAZCANO et al. 2022).

One of the most important measures to promote biodiversity that is gaining interest lies in the use of cover crops (CC) in the non-productive inter-rows between the vines. If managed properly with temporary or permanent CC, inter-rows have a great potential to host diverse plant communities and they can thereby cause several positive ecological effects (ABAD et al. 2021; GATTULLO et al. 2020). As WINTER et al. (2018) show, greened inter-rows can increase biodiversity and ES by 20%. Especially belowground biodiversity benefits from vegetation cover (BLANCO-PÉREZ et al. 2020). Moreover, extensively managed inter-rows are beneficial for a lot of pollinators due to the complex landscape and the floral resources (WILSON et al. 2018). Additionally, vegetation cover positively influences soil properties, such as organic carbon storage and water infiltration. It also mitigates erosion, since vineyards, especially those located on slopes, show a higher average soil loss rate and more degraded soil than other agricultural lands (PROSDOCIMI et al. 2016). In addition, ABAD et al. 2021 emphasize that CC can also increase the occurrence of species acting as natural enemies for vineyard pests.

Although CC are becoming more and more popular in recent years (WINTER et al. 2018), bare soil management by tilling and herbicide application is still a common practice in German and European vineyards, as winegrowers try to regulate competition for water and nutrients between the vines and the inter-row vegetation (HALL et al. 2020). However, recent research shows that grape yield can only be affected in drier climates, such as the Mediterranean regions (PAIOLA et al. 2020; WINTER et al. 2018). Even in the comparatively

dry east of Germany, the German biodiversity project *LIFE VinEcos*, completed in 2021, showed that CC had no negative significant impact on grapevine water stress and yield. On the contrary, positive effects on humus content and rooting have been demonstrated during the project time. It was also found that CC with wild plant flowering mixtures had lower soil erosion and higher biodiversity than those consisting of conventional flowering mixtures (mostly *Lolium perenne* and *Trifolium repens*). Similar observations were made by SCHMIDT et al. (2020).

Nevertheless, it is necessary to cut back the CC at a certain interval, otherwise, it will grow into the vines and also consume too much water (HOFMANN 2014). These cuttings can be conducted with different machines. Mulchers represent the most widespread working machine. With this technique, the plants are cut and crushed inside the mulcher, before the crushed material is left on the field (HECKER et al. 2022). On the one hand, the amount of phosphorus and potassium in the soil can be increased in this way and the mulch can prevent the soil from evaporation (ABAD et al. 2021). On the other hand, mulchers cause physical damage to several arthropod groups during the mulching process (HECKER et al. 2022). In terms of nature conservation, it can be more valuable if the greenery is cut with a mower and gets removed from the field to counteract widespread overfertilization. This method has a less negative impact on the fauna than mulching. The third management regime is the rolling of vegetation. Here, the roller bents down the CC. This allows its roots to grow into deeper layers, which improves the quality of the soil. Furthermore, the buckled plant layer is intended to protect the soil from evaporation and erosion (HOFMANN 2014).

A lot of research has already been done on management impacts on meadows and grasslands in general (cf. GILHAUS et al. 2017; RYSIAK et al. 2021). Here, different results show large differences concerning species composition and richness with different management regimes (cf. RYSIAK et al. 2021). In contrast, little is researched on how different types of inter-row management affect CC and its ability to provide certain ES in a viticultural context, especially in the long term. In addition, findings in viticulture can often only be interpreted regionally and German viticulture receives comparatively little attention in research (PAIOLA et al. 2020). Therefore, the management of inter-row vegetation in Rheinhessen, the largest German wine-growing region, is the focus of this bachelor thesis.

When, as in this thesis, small-scale vegetation analysis and spatiotemporal vegetation patterns are involved, UAV-based remote sensing has emerged as an appropriate method in recent years. Until a few years ago, remote sensing was only possible with earth observation

satellites and aircraft equipped with special sensor systems. With these systems, it was possible to achieve notable results of remote sensing in the agricultural context, since satellites are equipped with multi- and hyperspectral sensors that supply high temporal, spatial, and radiometric results (BOLLAS et al. 2021). However, when it comes to analysing within-vineyard variability, satellite remote sensing reaches its limits. For example, KHALIQ et al. (2019), MATESE et al. (2015) and WACHENDORF et al. (2018) show that the spatial resolution of the satellite imagery could not be directly used to reliably describe vineyard variability.

In this context, the introduction of Unmanned Aerial Vehicles (UAVs) as a carrier platform and the development of small and lightweight multispectral cameras have opened up new opportunities for remote sensing in environmental monitoring and other areas over the last two decades. Currently, agriculture represents the largest market and has the largest application potential for UAV-based multispectral remote sensing (OLSSON et al. 2021). There has been a strong increase in studies since the 2010s, making UAV applications for precision agriculture a fairly young field of research.

In contrast to satellite-based remote sensing, UAVs offer numerous advantages, but also some disadvantages, for agricultural and ecological purposes. On the one hand, satellites usually have a higher spectral resolution and consist of more spectral bands than multispectral cameras mounted on a UAV, allowing them to generate more vegetation indexes. On the other hand, UAVs achieve a much higher spatial resolution. While satellites offer a spatial ground resolution of tens of meters, UAVs can achieve a resolution of a few centimetres (VILLOSLADA PECIÑA et al. 2021). On top of that, UAVs are much more flexible in their application due to their reduced planning time, and they achieve to a large extent better temporal resolution (MATESE a. DI GENNARO 2018). For example, they make it possible to fly on any given day, since the flights do not necessarily require a cloudless sky (GRENZDÖRFFER 2019). This has the particular advantage that the reflection properties of the directly incident sunlight do not have to be corrected or modelled, which makes satellite products also process-intensive. In addition, UAVs can react flexibly to weather conditions and can be operated with comparatively low costs (OLSSON et al. 2021).

On this basis, UAVs have been already used for yield prediction (cf. MATESE a. DI GENNARO 2021), analysing grape quality (cf. CAMPOS et al. 2019), detecting pest infestations (cf. ALBETIS et al. 2017), monitoring vine health and drought stress (cf. BALUJA et al. 2012), or

detecting areas of high weed or invasive plant pressure (cf. CASTRO et al. 2020), allowing for precise management and efficient and site-specific use of agrochemicals in the vineyard. With these methods, the use of agrochemicals can be decreased significantly (LIBRÁN-EMBID a. GRAB 2020), which is again beneficial for biodiversity.

As mentioned above, the ability of vineyard landscapes to generate high biodiversity and to provide ES is closely linked to the right inter-row management. However, previous studies in the field of remote sensing have focused almost exclusively on the grapevine itself as the object of investigation, and UAV-based ecological research in a viticultural setting is still rare. Furthermore, there is a need for research on the question of how different management regimes influence inter-row vegetation. Therefore, this bachelor thesis presents a new methodological approach by investigating different management regimes in vineyard inter-rows by using UAV-based remote sensing. It thereby addresses the following research questions:

- a) Can UAV-based multispectral remote sensing be used to detect spectral differences between differently managed vineyard inter-rows?**
- b) How do different inter-row management regimes affect the inter-row vegetation and what spatiotemporal patterns can be identified?**

2. Materials and methods

The following chapter will present the materials and methods used in this thesis. After an overview of the study area and the investigated vineyards, the field equipment, and the data acquisition will be described. Further, the post-processing of the data and the statistical analysis will be addressed.

2.1 Study area

To answer the research questions mentioned above, three vineyards were investigated. They were all located in the wine-growing region of Rheinhessen in southwestern Germany (cf. figure 1). Area 1 (A1) ($49^{\circ}53'33.16''$ N, $8^{\circ}4'34.05''$ E) was situated in „Jugendheim“, while Area 2 (A2) ($49^{\circ}54'1.14''$ N, $8^{\circ}20'16.72''$) and Area 3 (A3) ($49^{\circ}57'17.25''$ N, $7^{\circ}57'19.06''$ E) were located in „Nackenheim“ and „Bingen am Rhein“, respectively. The height above sea level of the three vineyards ranged from 90 m (A3) to 160 m (A2) to 185m (A1). Detailed digital surface models of the three study sites can be found in appendix 3.

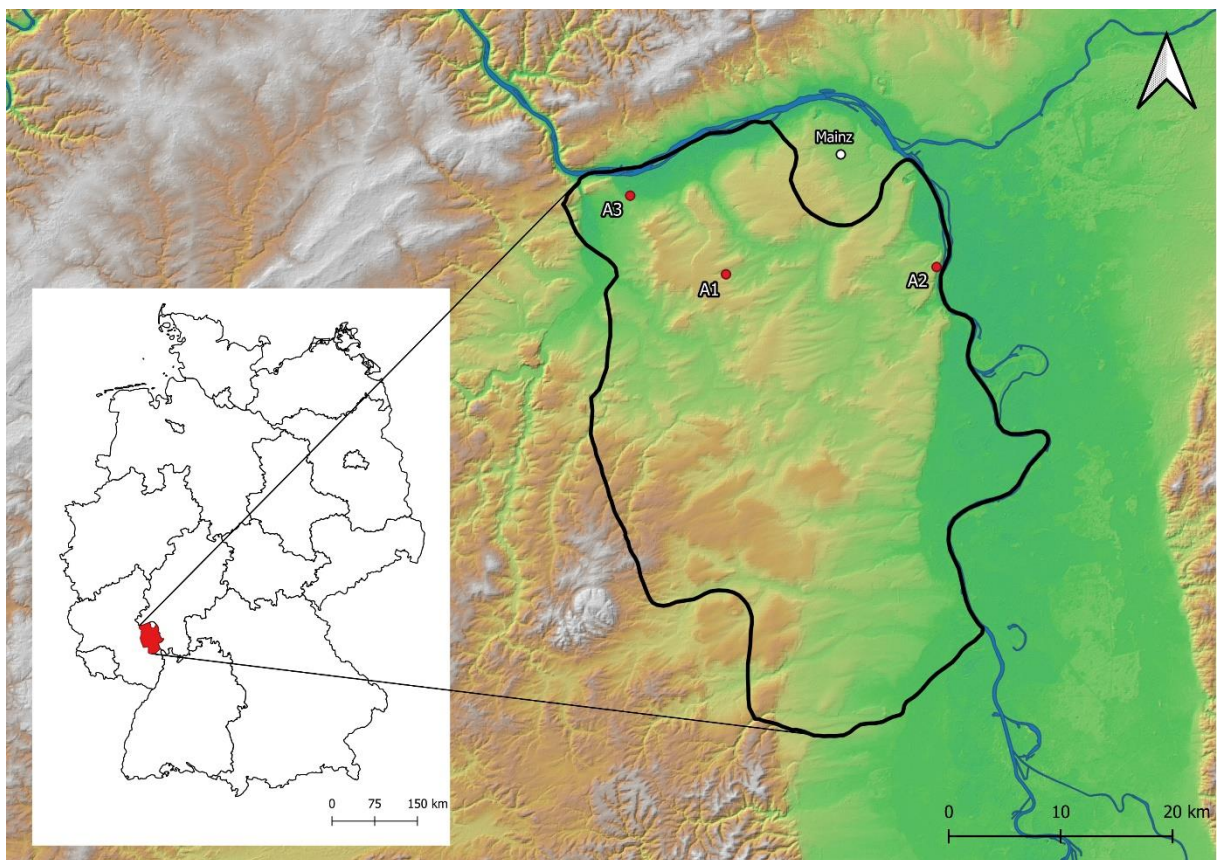


Figure 1: Location of the three investigated model vineyards (A1-A3). The black polygon represents Rheinhessen. The background is a DSM derived from Shuttle Radar Topography Mission (SRTM) data (Source: own representation).

With approximately 27.000 ha of vineyards, Rheinhessen represents the largest of the 13 wine-growing regions in Germany (DEUTSCHES WEININSTITUT 2022). It belongs to the federal state of Rhineland-Palatinate and lies in the wide triangle between Mainz, Worms, and Bingen. Rheinhessen is located completely on the left bank of the Rhine and is bordered by the Rhine to the north and east.

It developed into a region with a high level of agricultural land use up to the present day. This is underlined by the fact that it presents one of the least forested regions in Germany, with 5% of the total land area covered by forest (PREUB 2003). On the other hand, Rhineland-Palatinate has a total of 47% forested area (PREUB 2003).

Due to its protected location in the lee of Hunsrück, Taunus, Odenwald, and Nordpfälzer Bergland, Rheinhessen's climate is comparatively warm and dry and favours wine and fruit production (PREUB 2003). The average annual amount of precipitations is 530 mm (814 mm all over Rhineland-Palatinate). The average annual temperature of 10,5 °C is also higher than the average annual temperature of Germany (PREUB 2003). The average sunshine duration lies at about 1970 hours (average value for Oppenheim in the years from 1992 to 2019), and the vegetation period at about 280 days.

Geologically, Rheinhessen is closely linked to the history of the Oberrheingraben and is almost completely occupied by the Rheinhessische Tafel- and Hügelland (STEINGÖTTER 2005). This is a Tertiary stratified landscape that has predominantly the character of a frequently disintegrated plateau, whose level reaches between 250 and 320 meters above sea level (STEINGÖTTER 2005). According to the nature of the bedrock, the soils of Rheinhessen are often loamy and marly. However, predominantly loess soils occur, which go back to deposits of the Pleistocene (STEINGÖTTER 2005).

2.1.1 Model vineyards

The three investigated vineyards represent a selection from ten experimental vineyards of the biodiversity project "AmBiTo". This project aims to increase biodiversity in vineyards and vineyard landscapes by exploring and implementing different measures.

The three model vineyards can be seen in figure 2. They were selected based on different criteria. First of all, the inclination of the areas played a major role. Flat areas were chosen as far as possible because the majority of vineyards in Germany and especially in Rheinhessen do not consist of deep slopes but rather flatter vineyards, and therefore the vineyards provide a stronger comparison between each other. Additionally, with the drone,

flat areas can be better flown over, and the results can be less influenced by different climatic or edaphic variabilities influencing the vegetation (e.g., microscale differences in soil moisture content due to differences in slope steepness). In addition to this, areas were selected that have a similar size to generate better comparability between the model vineyards. The size of the three vineyards ranges from 0.32 ha (A1) to 0.43 ha (A3) and 0.44 ha (A2). Furthermore, the legal aspects were of high importance. To avoid illegal overflights (e.g., short distance to power lines, rails, or nature reserves), vineyards that may be legally overflown with the UAV were selected. Since a power line runs over A3, the power grid operator was contacted and obtained a flight permit in advance.

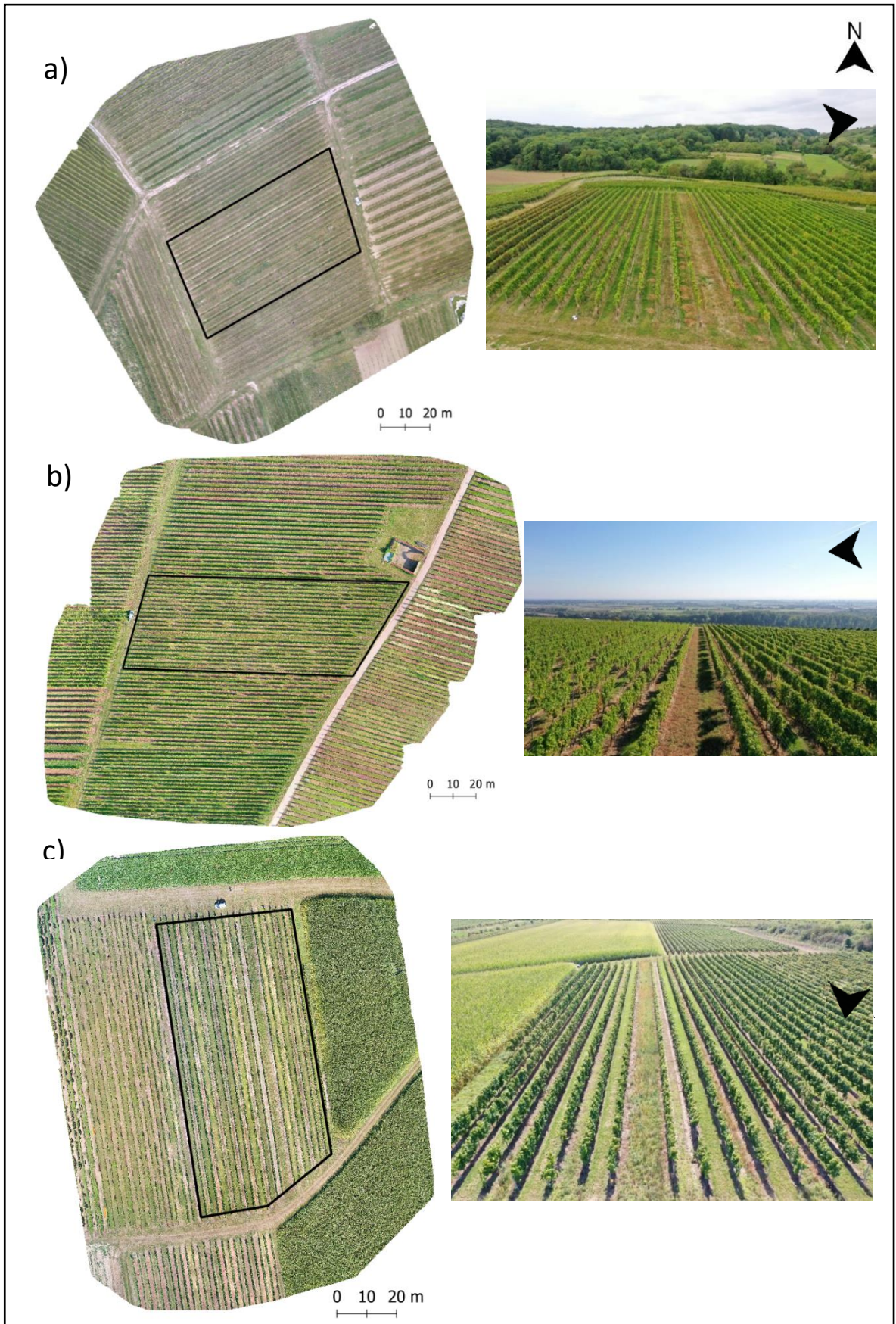


Figure 2: Overview of the three model vineyards. Orthophotos processed from the RGB camera of the Mavic 2 Pro (left) and landscape photos shot with the DJI quadcopter (right) of a) A1 b) A2 and c) A3. The black polygons on the orthophotos represent the location of the model vineyards (Source: own recordings).

2.1.2 Experimental design

Various flower strips with native wildflowers are being researched in the inter-rows of the ten experimental vineyards of the project “AmBiTo”. These experimental vineyards are sued to investigate which type of management allows permanent species-rich greening of the vineyard inter-rows. To answer this, each of the ten vineyards follows a similar experimental design. Figure 3 shows an exemplary structure diagram for A1. The diagrams for the other two model vineyards are presented in appendix 4.

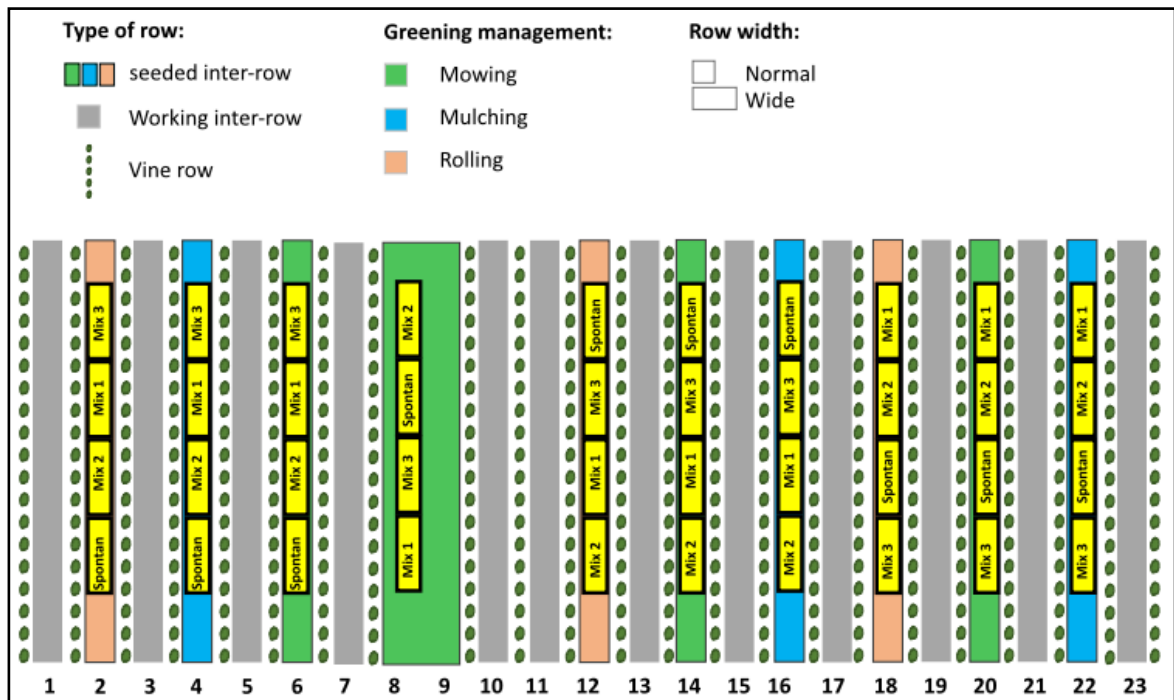


Figure 3: Experimental design of A1 (Source: own representation based on the AmBiTo-project).

Each model vineyard consists of 23 inter-rows in total. Ten of these inter-rows are sown with three different native wildflower mixtures, the other ones are working inter-rows that are not researched. The individual wildflower plots inside the rows have a length of 15 meters each. In addition, each inter-row has another 15-meter strip of spontaneous vegetation, so that each inter-row has a total length of at least 60 meters. If the inter-rows expand 60 meters, the remaining meters are either seeded with mixed vegetation or spontaneous vegetation. Note that, the differences between the individual flowering mixtures (1-3), or between these and the spontaneous vegetation are not investigated. This thesis focuses on the general effects of mix management types (mowing, mulching, rolling) on the inter-row vegetation.

The vegetation in the ten seeded inter-rows is managed with different machines. It is either mowed, mulched, or flattened with a roller. In each vineyard, there are four mowed, three

mulched and three rolled inter-rows. The cut material from the mowed inter-row vegetation gets removed, and that from the mulched inter-rows is left on the floor as mulch.

One inter-row in each plot is wider than the others. This inter-row is always mowed. For reasons of comparability, and to keep the row width constant within each vineyard, the wide inter-rows are not considered in this study, since they differ from other inter-rows (for instance in the input of solar radiation). Thus, in this study, three mowed, three mulched, and three rolled inter-rows are analysed in each model vineyard. Unfortunately, in rows 16 and 22 of A1, mulching was mistakenly carried out by the winemaker before the first flight. Therefore, these are also removed from the analyses.

The inter-rows were all sowed in the spring of 2021. The inter-row management (treatment) is carried out more than once over the vegetation period. A model vineyard is managed with the different management regimes in one day. The inter-row width and the sowing and treatment dates for the different model vineyards are shown in table 1. All flights were conducted before and after the second treatment of the year. However, it needs to be considered that there was already a similar initial treatment when it comes to discussing the results.

Table 1: Information about the different model vineyards (Source: own representation).

	A1	A2	A3
Inter-row width	1.2 m	1.6 m	1.5 m
Sowing date of seed mixtures	30.03.2021	31.03.2021	30.03.2021
Date of first treatment	25.06.2021	15.07.2021	28.06.2021
Date of second treatment	24.08.2021	07.09.2021	03.09.2021

2.2 Field equipment

In the field, different equipment was used to collect accurate aerial imagery. This equipment is presented in the following.

2.2.1 Ground Control Points

To enable accurate georeferencing of the orthophotos and ensure precise data analysis, five artificial ground control points (GCPs) were laid out on each vineyard. In general, GCPs are targets on the ground that have a known Global Positioning System (GPS) location and that can be easily identified in aerial images (FERRER-GONZÁLEZ et al. 2020). Thus, Real-Time Kinematic (RTK) GPS coordinates of the GCPs are measured in most cases. Since a RTK GPS receiver was not available at the time of the surveys, metal sticks were placed in the ground at the location of the GCPs after the first flight to allow the exact location of the GCPs to be rediscovered for the second flight.

The fabrication and placement of the GCPs were guided by existing literature (cf. ZIMMERMAN et al. 2020). Therefore, one GCP was placed in each corner of the model vineyards and one GCP was placed in the centre of the model vineyards. In addition, care was taken to have sufficient distance from any distorted parts of the image at the edge of the captured orthophotos. The GCPs were made of thick, black and white cardboard and had dimensions of 50x50 cm so that they formed a clear contrast to the otherwise green background and could be easily recognized on the orthophotos (cf. figure 4).



Figure 4: Ground Control Point on a model vineyard (Source: own photo).

2.2.2 UAV

The Mavic 2 Pro from the manufacturer DJI was used as the carrier platform for the multispectral sensor in this study. This represents a quadcopter with a weight of 907 grams and a maximum top speed of 72 km/h. In contrast to fixed-wing UAVs, quadcopters offer the advantage of a more stable image capturing process, resulting in a higher ground spatial resolution (MATESE et al. 2015). Thus, they are more suitable for vegetation mapping, which is shown by the results of BOON et al. (2017).

The Mavic 2 Pro is considered a robust and powerful quadcopter and, in addition to civilian applications, is also used in rescue operations and for various scientific and ecological purposes. VELLEUMU et al. (2021), for example, used the Mavic 2 Pro to collect river water samples for water quality assessment. The drone also has an RGB camera from the manufacturer Hasselblad, whose images can be seen in figure 2.

2.2.3 Multispectral camera

The UAV was complemented by the Parrot Sequoia multispectral camera, which was specifically designed for vegetation mapping and other agricultural purposes such as biomass estimation (HAN et al. 2019; KOPAČKOVÁ-STRNADOVÁ et al. 2021). The camera consists of one RGB sensor with a 4608 x 3456-pixel sensor and a focal length of 4.88 mm (FRANZINI et al. 2019). Moreover, the Sequoia consists of four separate multispectral sensors with global shutters that enable the camera to capture images in the green, red, red-edge, and near-infrared wavelength bands (cf. table 2). Their resolution is 1280 x 960, with a focal length equal to 3.98 mm.

Table 2: Wavelengths of the different Parrot Sequoia bands (Source: own representation based on FRANZINI et al. 2019).

Band	Green	Red	Red Edge	Near-Infrared
Wavelengths (nm)	480-520	640-680	730-740	770-810

Additionally, the Parrot Sequoia features a separate sunshine sensor calibrating the measured spectral radiation by the main sensor. The sunshine sensor has a hemispherical field of view that measures solar irradiance in the same spectral bands as the four image sensors to allow accurate results under different weather conditions (OLSSON et al. 2021). It also consists of a GPS receiver and IMU (inertial measurement unit) that allows the calculation of the position and orientation of the sensor during the flight (OLSSON 2021). The two parts of the

camera were attached to the drone by a special mount that was designed by „DroneExpert.nl“.

As the results of OLSSON et al. (2021) show, the sensitivity of the Parrot Sequoia can be affected by camera temperature and atmospheric influences. According to their notes, the sensor was warmed up before the individual flights and images of the reflectance calibration panels were taken before each flight to ensure accurate image collection.

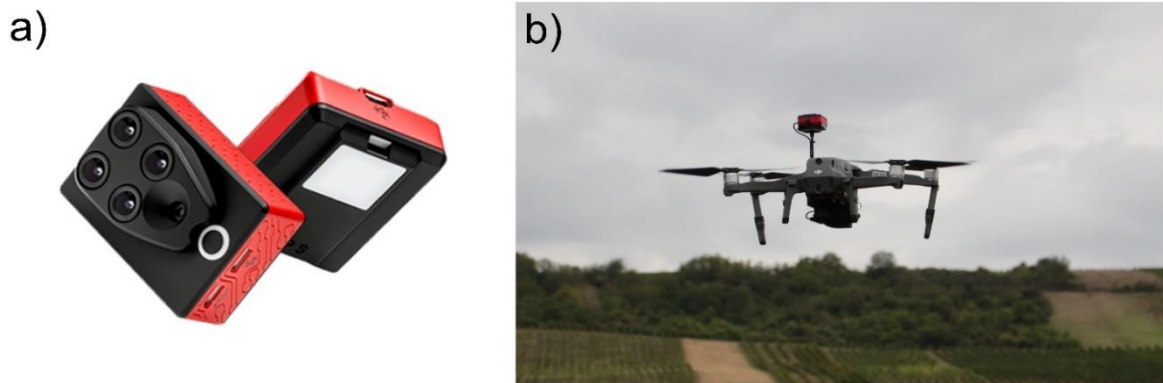


Figure 5: The Parrot Sequoia multispectral camera and sunshine sensor (a) and the DJI Mavic 2 Pro quadcopter with the attached Parrot Sequoia (b) (Source: <https://www.parrot.com/us>; own recording).

2.3 Flight Planning

Before the flights were carried out, flight plans were created for each vineyard using the Pix4Dcapture application from the manufacturer Pix4D. The software was installed in advance on the smart controller of the DJI drone. With the application, the flight area was defined, which was chosen large enough to cover all the required areas (inter-rows with seed

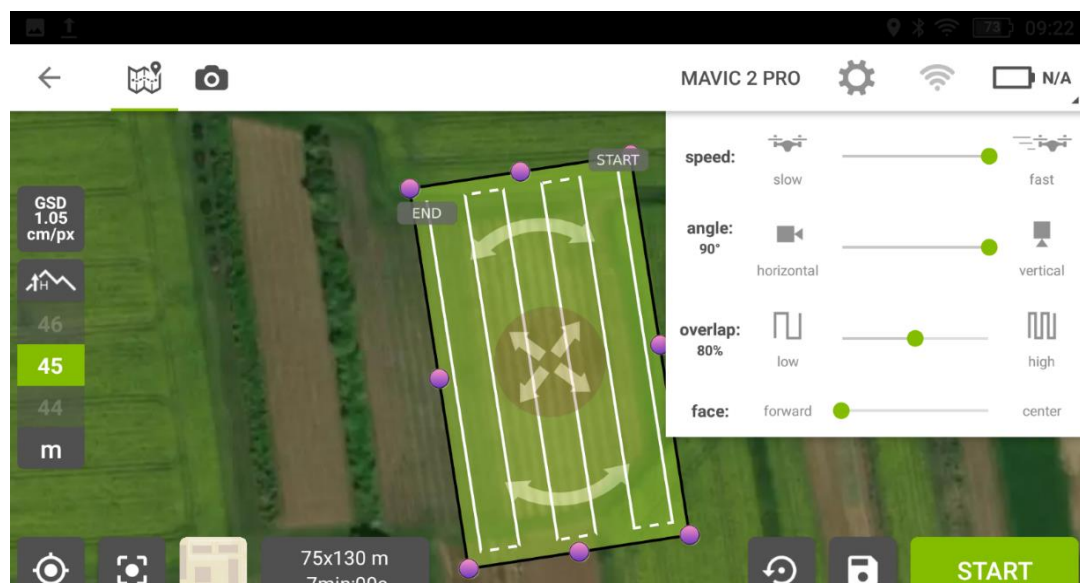


Figure 6: Screenshot of the Pix4DCapture application during the planning of a flight over A3 (Source: own representation).

mixtures and working inter-rows). In addition, the flight altitude, the take-off and landing point, the flight speed, and the image overlap were defined with the help of this software. The flight speed was about 3.6 m/s during every flight. According to recommendations from various studies (cf. JIMÉNEZ-JIMÉNEZ et al. 2021; ALBETIS et al. 2017), the image overlap for all the flights was set at 80%, so that an accurate orthophoto could be processed from the raw data later. An exemplary screenshot of the flight plan from A3 is presented in figure 6. The previously adjusted settings can be seen on the right side of the screenshot. The detailed flight routes for the individual model vineyards can be seen in appendix 5.

2.4 Image acquisition

To investigate how the management types affect the vegetation, two flights were taken on each of the three model vineyards. The first flights (A1.1; A2.1; A3.1) are considered the reference, and it was taken immediately before (on the same day) or up to 5 days before the inter-row management. The second flights (A1.2; A2.2; A3.2) were taken 15-19 days after the inter-row management to avoid stormy and rainy weather conditions. The individual time shifts came about because the flight days were bounded to the winemaker's management days. Information about the individual flights can be seen in table 3.

Table 3: Detailed information about the individual flights.

Flight	Date	Time	Weather conditions	Flight altitude	Flight duration	Number of images*	Covered Area (ha)
A1.1	20.08.2021	02:00 pm	cloudy	45 m	6 min	181	1.53
A1.2	10.09.2021	10:30 am	cloudy	45 m	6 min	179	1,60
A2.1	02.09.2021	09:30 am	mostly sunny	45 m	8 min	247	1,68
A2.2	23.09.2021	10:30 pm	sunny	45 m	8 min	248	1,87
A3.1	03.09.2021	12:45 pm	sunny	45 m	5 min	161	1,00
A3.2	23.09.2021	12:45 pm	sunny	45 m	5 min	160	1,07

* Number of images for each of the five sensors (RGB, Green, Red, Red Edge, NIR)

It was tried to conduct the flights in the midday period from 10 am to 2 pm, as this is common practice (cf. ALBETIS et al. 2017). However, this was not always possible. For example, the

flights on A2 were taken a little earlier to avoid too much shadowing of the west-east-oriented vines. Canopy shadowing was not a challenge on the west-east oriented A1, as it was flown on cloudy days. The flight altitude was always set to 45 m above ground level (AGL). This comparatively low height was chosen as a compromise between spatial resolution and a manageable amount of data.

2.5 Image processing

Next to the already presented hardware used in this thesis, different software was needed. From the single raw imagery, high-resolution orthophotos and DSMs were created with the open-source photogrammetry software WebODM (OpenDroneMap, version 1.9.3). This software is a user-friendly alternative to the, for scientific purposes well-established, commercial software Pix4D and Agisoft Metashape. Nevertheless, several studies, such as GROOS et al. (2019), have already proven the suitability of WebODM for research and academic education in various geoscientific disciplines. WebODM uses Structure from Motion (SfM) technology to process the individual orthophotos. SfM is a photogrammetric method to reconstruct three-dimensional structures (e.g. terrain models) from overlapping image sequences (CASTRO et al. 2021). It is used in several scientific or economic disciplines, such as architecture and agricultural mapping.

The multispectral orthophotos processed in this way were further used to calculate *Normalised Difference Vegetation Index* (NDVI) images of the model vineyards. The NDVI is the most commonly used vegetation index for agricultural and viticultural purposes and it has already been used for decades in the research field of remote sensing and environmental monitoring (HUANG et al. 2021). It is widely used as a direct indicator of vegetation growth and health, since it strongly correlates with the photosynthetic activity and vitality of the plants. It is thus a reliable indicator for characterizing the condition of vegetation (ABOUTALEBI et al. 2018).

To start processing, the raw data had to be uploaded to the software first. Secondly, the high-resolution option was set, before the processing was started. Depending on the number of images that had to be reconstructed, processing took about 1-2 hours for each of the six processed orthophotos. Since WebODM corrects the invited raw data itself, no pre-processing, such as radiometric correction, was necessary before starting the reconstruction of the aerial imagery. After the processing, the orthophotos were exported as a TIF file.

The QGIS (version 3.12.3) *Georeferencer* plugin was then used to georeference small deviations of the two images (before and after the management was applied a second time) from the same model vineyard, if necessary. This was done using the GCPs so that the two images were exactly congruent and the NDVI data could be precisely extracted for the two different times.

To turn the georeferenced multispectral imagery into NDVI maps, the raster calculator was used in QGIS. The NDVI was computed by the following equation:

$$NDVI = \frac{NIR - RED}{NIR + RED}$$

The value range of the NDVI is -1 to 1. Values of less than -0.1 are usually assigned to water surfaces. Values ranging from -0.1 to 0.1 characterize barren areas, snow, or sand. Values from 0.1 to 0.4 correspond to grassland and shrub, whereas values ranging from 0.4 to 1 are attributed to dense vegetation. Values close to 1 correspond to tropical rainforests (BOLLAS et al. 2021, YA'ACOB et al. 2014).

2.6 Statistical analysis

To answer the research questions, the NDVI values of the 60-meter plots, in which the cover crops are located, had to be extracted from the image data, for both times (before and after the inter-row management). For this purpose, a shapefile line was first generated on the processed orthophotos along with the 60-meter plots in the middle of the rows. A buffer with a total width of 40 cm was created around this line in the next step (cf. appendix 9). This width was chosen to ensure that only the vegetation and not the soil area kept open by herbicides at the edges of the inter-rows was included in the analysis (cf. appendix 1). This resulted in a pixel count of approximately 9500 inside each of the 60-meter buffers. Then, random points were created inside the buffers. Based on these random points, approximately 10% of the pixel values were extracted, as one random point extracts one NDVI value. This procedure was repeated for both NDVI images of a model vineyard (before, and after the inter-row management) with the same random points. Using the *Point Sampling Tool* plugin in QGIS, the NDVI value extracted from each random point was supplemented with the inter-row number, the management regime and the time (before, or after the inter-row management). The obtained pixel values were exported in a CSV file from QGIS. In this way, a transparent data set for each model vineyard was created, which was invited into

Microsoft Excel 2019 and RStudio (version 4.0.2, R Development Core Team 2020) for further statistical analyses.

The results of NDVI values at the different times and for the different management regimes (mowing, mulching, rolling) were visualized using tables, histograms, and boxplots created in Microsoft Excel and R. To test i) whether effects on the vegetation cover by inter-row management, in general, can be detected by differences in NDVI values and ii) if the strength of the effects on the vegetation cover depends on the management regime, a two-factor covariance analysis (with the factors of time, management regime, and their interaction) was performed in R. This analysis was performed for each model vineyard separately. This relates to the spatial component of the thesis to see if the effects follow a general pattern, or if they are spatially explicit. The significance level was set to $\alpha = 95\%$. As a prerequisite, the data set was checked for normal distribution before. This was done using the `ggplot2`-function in R. The R scripts for the performed analyses and the results of the check for normal distribution can be found in appendix 7 and 8.

3. Results

In the following section, the results of the thesis will be described. At first, the processed aerial imagery and the calculated NDVI images will be evaluated. Secondly, the spatiotemporal vegetation patterns will be presented.

3.1 Aerial imagery

In total, six RGB and six multispectral orthomosaics were processed with the WebODM software. Figure 7 shows an example of A3 before the inter-row management was carried out. Looking at the multispectral imagery, the individual images of the four spectral bands (Green, Red, Red Edge, NIR) were output on top of each other in one image, resulting in a false colour image (cf. figure 7, right image). The vines, as well as the inter-row areas, are well recognizable. In addition, the wider inter-row stands out. Also visible are purple areas with lots of vegetation and lighter areas indicating a high open soil content. Taking a closer look at the images, one can clearly distinguish the sowed inter-rows from the working inter-rows. The blossoms of the CC are also recognizable.

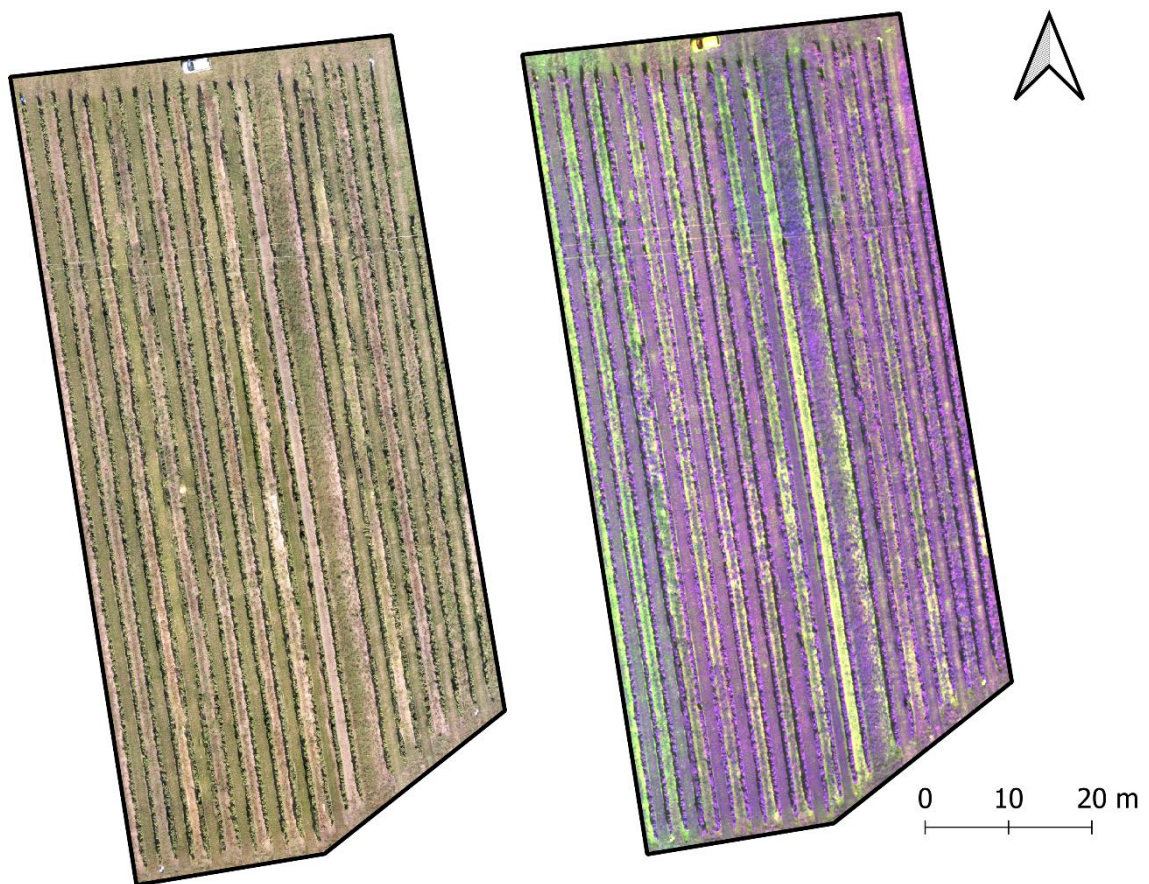


Figure 7: Example of the processed RGB (left) and multispectral (right) imagery (A3 before the inter-row management) (Source: own representation).

The GSD lies at about 4 cm in all multispectral orthophotos (cf. table 4). In contrast, the GSD of the RGB imagery taken from the Parrot Sequoia lies at about 1 cm.

Table 4: Ground Sampling Distance (GSD) of the RGB and multispectral orthophotos (Source: own representation).

Flight	A1.1	A1.2	A2.1	A2.2	A3.1	A3.2
GSD of RGB imagery	1.1 cm	1.2 cm	1.2 cm	1.2 cm	1.1 cm	1.2 cm
GSD of multispectral imagery	4.0 cm	4.1 cm	4.1 cm	4.2 cm	4.0 cm	3.9 cm

Figure 8 shows the NDVI images calculated from the multispectral orthophotos. An enlarged view of the individual NDVI images can be found in appendix 6. As in the multispectral orthophotos presented above, the vine rows and the inter-row area can be easily distinguished from each other. The CC can be seen too. In the before-after comparison, the wider row is particularly conspicuous, as it appears with markedly lower NDVI values after mowing than before the mowing. Also conspicuous are areas with a low NDVI in the understock area, i.e. areas with bare soil typically caused by the chemical herbicides that are used on all of the model vineyards.

In some cases, areas with a higher NDVI are visible in the second images (after the inter-row management was conducted). This is caused by the working rows, which have regenerated in the period, and the vines, which have ripened in the period.

However, in order to recognize and prove structural vegetation patterns, deeper data analysis is required, which was also carried out in this bachelor thesis and will be discussed in the next chapter.

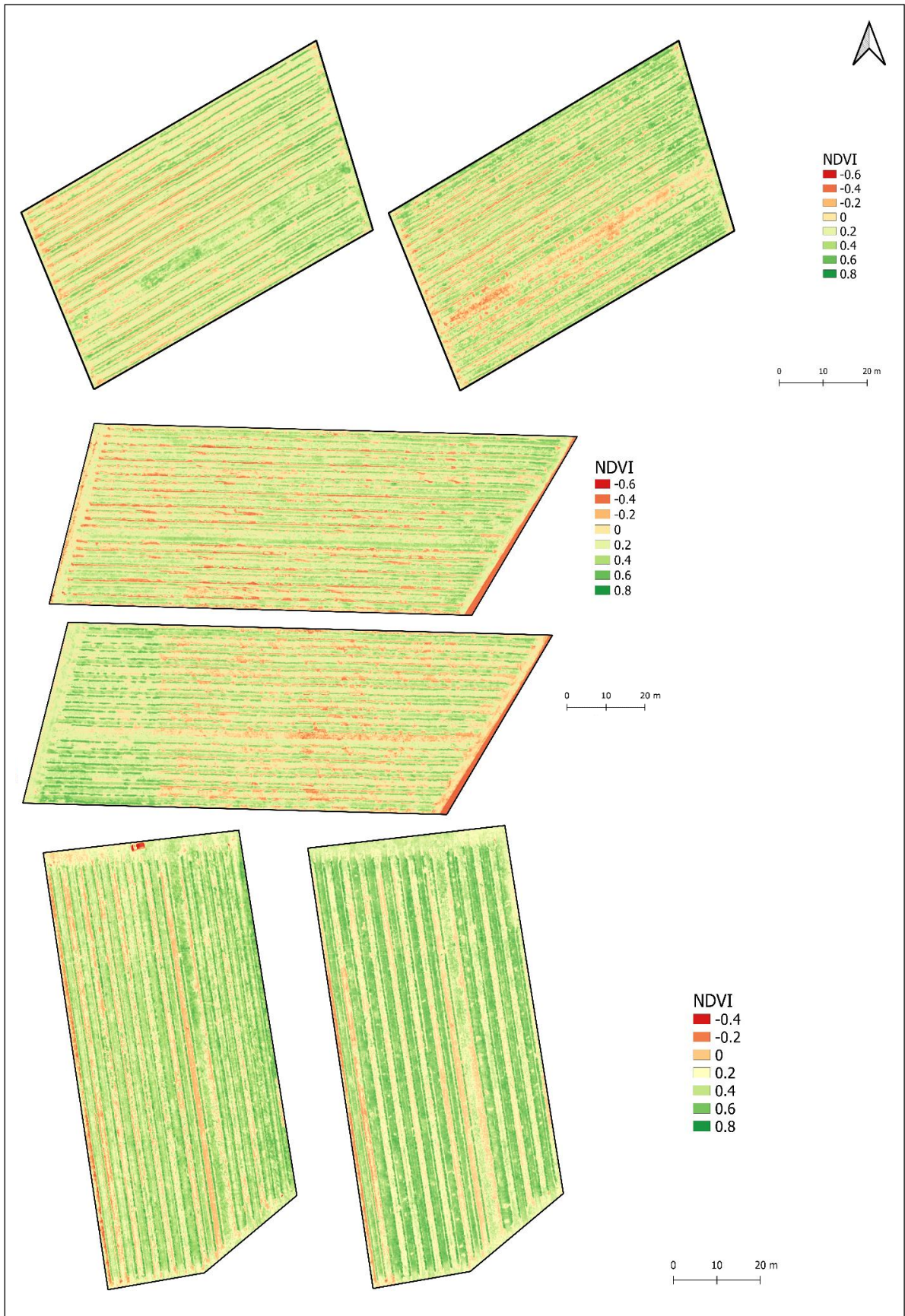


Figure 8: NDVI images of the three model vineyards for each of the individual flights (Source: own representation).

3.2 Spatiotemporal management effects

As can be seen from Table 5, a total of 12198 data points were included in the statistical NDVI analysis. There were measurable differences between the recording times and management regimes.

Looking at the distribution of the NDVI values at different times (figure 9), we see a shift in the distribution. At the time before the inter-row management (before treatment = BT), the values are in a range between -0.31 and 0.67. 96% of the values are in the range between 0 and 0.6. About 3% of the values are in the minus range and 0.56% of these are below -0.1. About 0.5% are above the value of 0.6. Most of the values are in the range between 0.2 and 0.4 (5771 values). 3429 values are in the range between 0 and 0.2, followed by the value range between 0.4 and 0.6 with 2561 values.

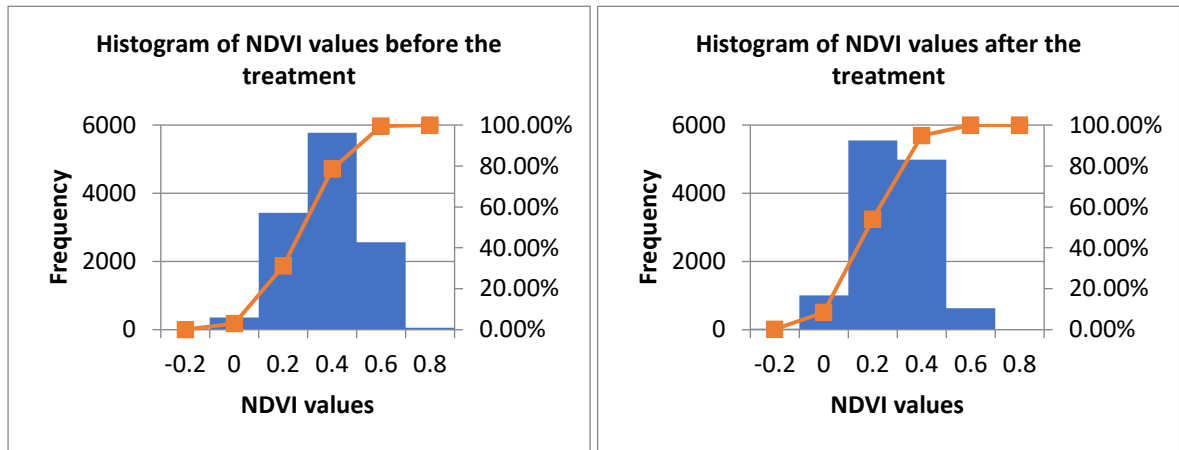


Figure 9: Histograms and cumulative frequencies of NDVI values before and after inter-row management (Source: own representation).

After the inter-row management (after treatment =AT), the range of values extends from -0.26 to 0.61. At this point, more than 91% of the pixel values are in the range between 0 and 0.6. With 9%, more values are in the minus range than BT. Of these, 2.26% are below -0.1. In addition, only 2 pixels are above the value of 0.6, which accounts for 0.02%. Unlike before the treatment, most of the values after the treatment are in the range of 0 to 0.2 (5544). This is followed by the range from 0.2 to 0.4 (4984). This time, only 633 values (5.2%) are in the range from 0.4 to 0.6.

Looking at the descriptive statistics in table 5, it can be seen that the vegetation has a lower mean NDVI at the AT period compared to BT. The difference between the two mean values is 0.09 across all areas. This decrease can be seen in all model vineyards. However, the decreases in the three model vineyards are varying in magnitude. While the difference for

A1 is 0.22, it is 0.06 for A2 and only 0.02 for A3. The median values of both times show a similar pattern as the mean values.

The different height of the mean values is also interesting. In the BT period, the flowering strips on A1 reach an NDVI mean value twice as high as on A2. A3 also has a much lower mean value than A1, with a mean NDVI of 0.25. In the AT period, however, the differences between the mean values are less pronounced. Here it is even the case that A3, with an NDVI of 0.23, has a higher mean value than A1 and A2. A2 has the lowest of the three values with 0.14.

In contrast to the mean value comparisons, there is no clear picture of the minimum and maximum values. Here the smallest value is even in the BT period. The maximum value, however, is in the AT period somewhat lower than BT. It is also noticeable that the values AT scatter less around the mean value than BT. While the standard deviation in the BT period lies at 0.15, it is 0.13 in the AT period. Only A1 deviates from this pattern. Here the standard deviation in the AT period is 0.17, while previously it was 0.12. However, there are some statistical outliers in lower ranges (cf. figure 10).

Table 5: Descriptive statistics of the NDVI analysis of the model vineyards before the inter-row management (BT) and after the inter-row management (AT).

	All areas		A1		A2		A3	
	BT	AT	BT	AT	BT	AT	BT	AT
n	12198	12198	3414*	3414*	4392	4392	4392	4392
Mean	0.28	0.19	0.41	0.19	0.2	0.14	0.25	0.23
Median	0.27	0.19	0.42	0.19	0.22	0.15	0.24	0.23
Minimum	-0.31	-0.26	-0.16	-0.26	-0.31	-0.24	-0.12	-0.12
Maximum	0.67	0.61	0.67	0.61	0.49	0.49	0.61	0.67
Standard deviation	0.15	0.13	0.12	0.17	0.11	0.1	0.14	0.1

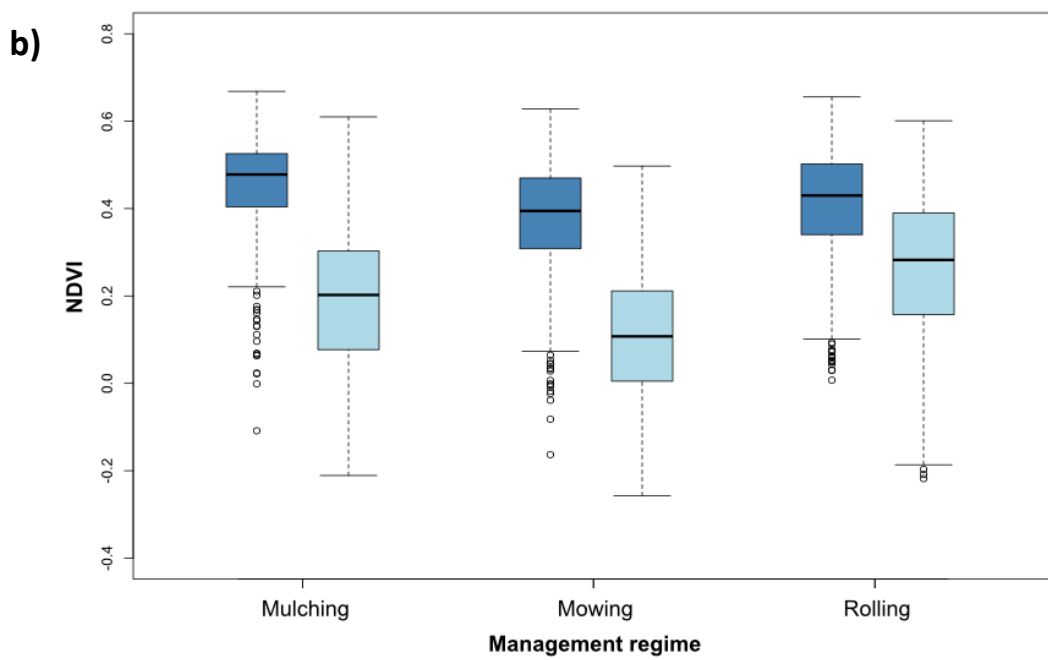
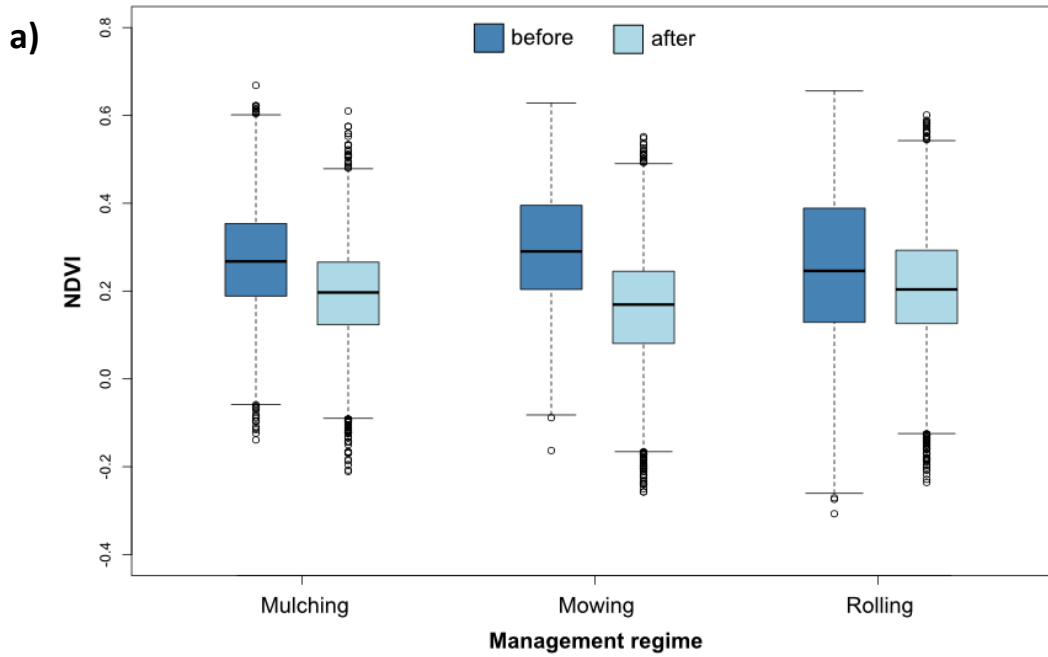
*Two mulched inter-rows had to be removed from the analysis (cf. chapter 2.1.2)

If we add the different management regimes (mowing, mulching, rolling) to the analysis, we also get interesting results, which can be seen in figure 10. First of all, it must be noticed that, after the treatment, the mean of the NDVI values has visibly decreased for each management regime, although to different degrees. Thus, the greatest decrease is observed for mowing (-0.14), followed by mulching (-0.08) and rolling (-0.04). This pattern is also seen in all three vineyards, with rolling standing out the most from all the management

regimes. On A3, the rolled inter-rows even show a slightly higher NDVI in the AT period than in the period before the treatment.

It is also evident that in the BT period, rolling has the lowest mean value of the three management types, while it has the highest in the AT period. In the case of mowing, the opposite is true: BT it has the highest mean value, while AT it has the lowest.

Differences can also be seen concerning the measures of scatter. Thus, the standard deviation for both time periods (BT and AT) is highest for rolling (0.16), followed by mowing (0.15), and mulching (0.13). By far the highest deviation is found for rolling in the BT period. Furthermore, before the treatment, the values of the mulched and the mowed inter-rows scatter less in the negative value spectrum than in the period after the treatment, whereas the rolled inter-rows have even more negative values in the period BT than after the treatment.



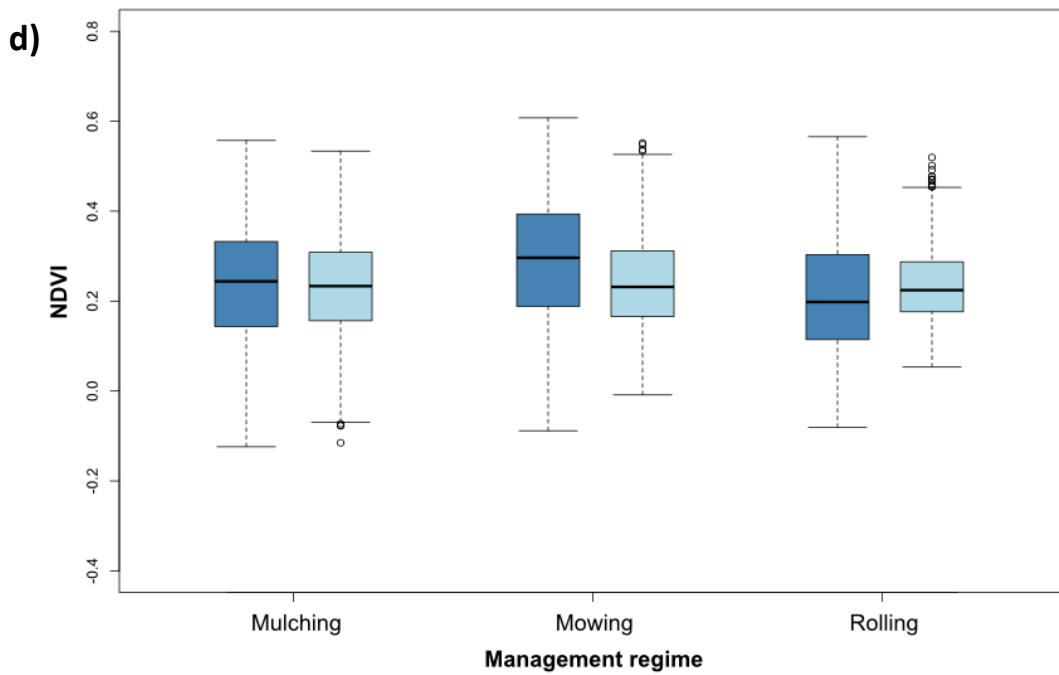
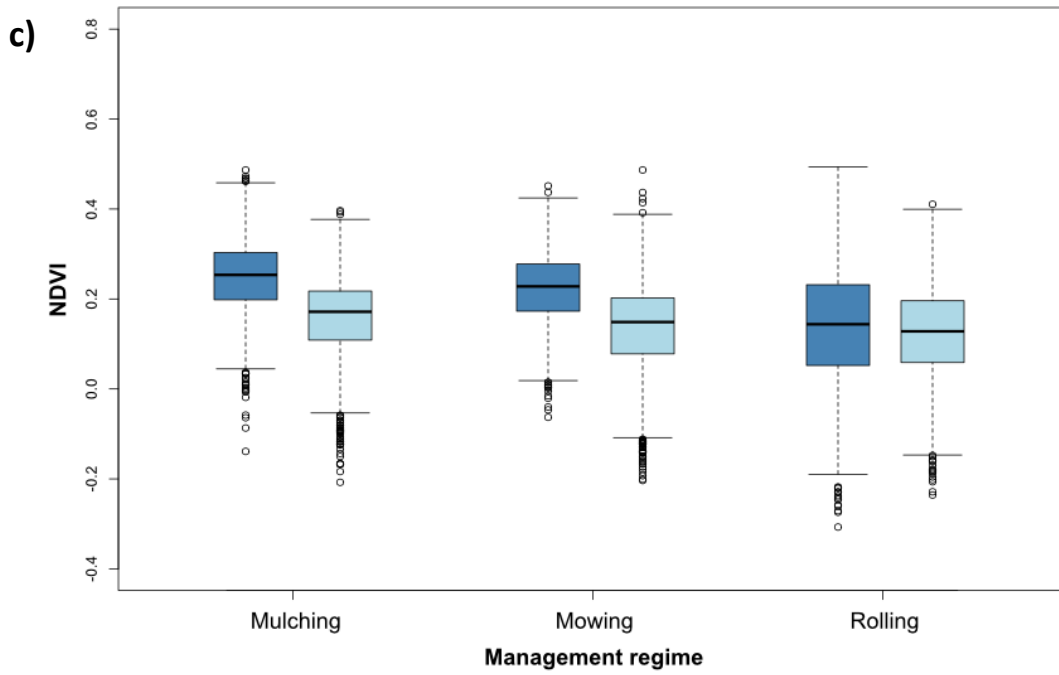


Figure 10: Boxplots of NDVI values as a function of time and management regime of a) all areas, b) A1, c) A2, d) A3.

The results of the conducted covariance analysis confirm the picture that emerges from the boxplots. On all model vineyards combined, there is a significant difference in terms of NDVI between the two times ($F_{1,12197} = 2521.27$; $p = <0.001$). This shows that the NDVI is significantly higher in the BT period than in the AT period. Furthermore, there is no significant difference in NDVI values between the management regimens when considered as a single factor ($F_{2,12196} = 1.8$, $p = 0.165$). However, when the interaction effect between time and management regime is considered, it is significant (time * management regime: $p = <0.001$). This means that the differences in NDVI values between the BT period and the AT period are dependent on which management regime has been applied. A table with the results of the analysis for each model vineyard can be found in appendix 10. The pattern found across all areas is consistent for each model vineyard.

4. Discussion

The presented results show that it is possible to use UAV-based aerial imagery to create high-resolution orthophotos which are capable of indicating the condition and response of inter-row cover crops to different management regimes in viticulture. The results show a pattern that can be statistically proved, as the NDVI values were significantly lower after the implementation of the inter-row management than before across all areas. Thus, the method is suitable for detecting spectral differences related to different management regimes across vineyards in the same vine-growing region. However, some differences in the magnitude of this pattern were found between the single vineyards. Furthermore, the results show that rolling is, with regard to its effect on the vegetation, the least intense of the three management types investigated in this bachelor thesis. This pattern was also the same across all three model vineyards.

In the following chapter, the results will be discussed and put into the context of current research. In addition, the methodological limitations and external influences will be addressed.

4.1 Image evaluation

Overall, the results demonstrate that the open-source application WebODM, in combination with the drone and multispectral sensor used, is suitable for generating orthophotos and thus analysing small-scale structural differences in vineyards. This is consistent with the results of several studies that have compared WebODM with commercial photogrammetry

software. For example, PELL et al. (2022) show that, despite having some poorer results in other fields, WebODM is even ahead of the other programs in some categories, such as geographic accuracy. CHANGSALAK a. TIANSAWAT (2022), as well as VACCA (2019), also give WebODM solid scores for environmental monitoring compared to other providers, such as DroneDeploy and Pix4D.

The generated orthophotos can be processed quickly and accurately with the settings made. Only at the edges of the orthophotos, some distortions are visible. This is a well-known phenomenon that HOLMAN et al. (2019) have already encountered. This is probably related to the Structure from Motion technology. As KRAUS (2004) describes, various error influences in the photogrammetric method can cause positional inaccuracies and distortions to appear on the orthophotos. He says that these inaccuracies usually increase from the centre of the image outward in a radial direction, as in the processed images of this thesis. However, this was taken into account in the methodology, so that an area was recorded that went beyond the area of the vineyards (cf. figure 2). Thus, the distortions do not pose a problem for the applied statistical analysis of the model vineyards, which are located in the centre of the image.

The GSD of the processed data is within the expected range for the UAV flight altitude. As described by FRANZINI et al. (2019), the GSD of the RGB data derived from the Parrot Sequoia should be about 1.9 cm at an altitude of 70 meters AGL. For the multispectral images, the GSD should be 6.8 cm at 70 meters AGL (FRANZINI et al. 2019). If these data are adjusted to the flight altitude of 45 meters AGL set in this thesis, the GSD of the orthophotos generated with WebODM is even slightly below the expected values.

4.2 NDVI evaluation

Looking at the results of the distribution of NDVI values and comparing them to the NDVI classifications from existing literature, most of the pixel values are within the expected range. The majority of the values, both BT and AT, are in the range of 0.1 to 0.4, a range usually assigned to shrubs, grasslands and meadows (BOLLAS et al. 2021). However, a significant portion of the values is also in the range from -0.1 to 0.1, which characterizes open ground or stones (BOLLAS et al. 2021). This can be explained by the high proportion of bare soil in the alleys in some cases (personal observation during field surveys). Since the flower mixtures were sown only four to five months before the overflights and the

spontaneous vegetation has only been able to grow since then, it is still comparatively sparse (cf. appendix 2). It will become increasingly dense over the next years.

Nevertheless, there are also some unusual pixel values. For example, some of the values (0.56% before the treatment and 2.26% after the treatment) are below the critical value of -0.1, which is actually only assigned to water surfaces (YA'ACOB et al. 2014). Here, the sensor seems to underestimate the open ground areas or the cut vegetation. This is surprising because BOLLAS et al. (2021) conclude that the measured NDVI values of the Parrot Sequoia camera are often even higher than the NDVI values of Sentinel-2. Some values are also found in the range above 0.4. This range is normally categorized as dense vegetation (BOLLAS et al. 2021). However, the values of UAV-based aerial imagery also scatter more than the values derived from satellite data, because of the different spatial resolutions of the platforms (BOLLAS et al. 2021). This factor could explain the wide distribution of some values (into the low and high ranges). In addition, the original classifications in the literature probably refer mostly to satellites as platforms.

Also noticeable is the left area on the NDVI image of A2.2, which shows greener vines. This could indicate an error in the sensor recordings. However, it is more likely that artificial irrigation by a sprinkler on the bordering parcels has caused the NDVI values to be higher here, as there were no clouds that could have changed the reflectance characteristics during the flight. Soil mounding is unlikely, since A2.1 does not show this pattern.

4.3 Spatiotemporal management effects

The findings of this bachelor thesis show that the CC have the highest NDVI values after rolling and the rolled CC are thus the most photosynthetically active and healthy. These findings are in line with the statements of HOFMANN (2014), who describes rolling as a management regime that has comparatively low impacts on the flora and fauna of the vineyard.

It is particularly striking in this context that the rolled CC show the lowest NDVI values before management. This could be due to a possible increased number of blossoms in the rolled alleys, as opposed to the mulched and mowed CC. As SHEN et al. (2009) and SHEN et al. (2010) demonstrate, a high number of blossoms reduce NDVI, as they change the reflectance characteristics of the vegetation cover. To this end, one must also consider that one initial treatment (the first treatment after seeding, see table 1) has already taken place a

few months earlier. Due to the low-impact rolling management, more flower heads may have developed here after the very first management cycle than in the other row types and, thus, the blossoms could have decreased the NDVI before the treatment. There was slightly more flower-rich material in all of the rolled inter-rows than in the other inter-rows (personal observation during field surveys). Furthermore, the inter-rows could also have been in a different phenological state and the rolled inter-rows might have already been a little more faded due to the very first initial treatment.

There are differences between the three model vineyards concerning the expression of the spatiotemporal patterns. For example, A1 showed the largest before-after NDVI decrease, while A3 showed the smallest changes. In this context, it must be taken into consideration that the vineyards were not all flown over at the same temporal distance after the management was carried out. Due to the weather conditions, A3 was flown over after the second treatment 3 and 4 days later than the other two model vineyards. Thus, the cover crops here had more time to regenerate.

Additionally, certain microscale and regional factors may affect the cover crops, resulting in vineyard-specific differences. For example, GILHAUS et al. (2017) examined grassland for various management effects:

“However, it also became obvious that vegetation composition was not strictly distinguished by management alone. Local and regional characteristics such as soil conditions, size of the grassland species pool or land-use history, often played a more prominent role than land use alone. [...]. The dependency of a certain management scheme on site-specific environmental factors such as soil fertility, further complicated the clear separation of management effects from those of the environmental background” (GILHAUS et al. 2017, p. 379).

The cover crops therefore have, depending on soil conditions, microclimate, land-use history, and previous management, different densities and different species compositions between the model vineyards (cf. appendix 1). In addition, there are some variations in actual management between the model vineyards, since they are managed by different winegrowers. The winegrowers do not use exactly the same vehicles and machinery models. Furthermore, all winegrowers use herbicides in the understock area, but to various degrees. This was reflected in the inter-rows in a different proportion of open soil near the understock areas (cf. appendix 1). The model vineyards also differ in species composition such as in the proportion of grasses and herbs. For example, grasses and herbs respond differently to

management regimes. Species composition also affects the spectral signature of the green cover, and thus the NDVI values, since different species have a different spectral reflectance (PERSSON et al. 2018). This must always be considered when interpreting the results. These site-specific differences in the vegetation density, the bare soil portion and the vitality of the greening could also have caused the different mean values between the three model vineyards. In this context, the comparatively low values on A2 are noteworthy. This could be related to the fact that the inter-rows on A2 were partly shaded during both flights. As ABOUTALEBI et al. (2018) show, shadowing can influence the performance of the NDVI and lead to reduced values in vineyards due to low reflectance. However, since all inter-rows were shadowed constantly to the same degree, the impact on the methodology can be neglected.

Moreover, this study has only a comparatively low temporal resolution. To truly measure spatiotemporal vegetation changes over a long period, a methodology that collects data over the entire vegetation period would be needed (cf. TÓTH 2018). In addition to that, two mulched inter-rows on A1 had to be removed from the analysis, because the winegrower mistakenly mulched them before the first flight was carried out. Thus, there was a reduced number of samples on A1, which could have affected the overall results.

Nevertheless, this thesis aimed to investigate whether the UAV-based multispectral remote sensing method can be used to identify measurable patterns of plant health in the inter-rows and to measure how these patterns are expressed between the different management regimes. In this respect, this bachelor thesis provides clear and measurable results. Although the NDVI cannot be used to make direct statements about biodiversity (HUANG et al. 2021), the results can be indirectly related to the findings of HOFMANN (2014). The results make it clear that rolling is the most suitable method to protect the flower-rich material and enable high biodiversity. Mulching should be avoided from this point of view because insects and arthropods largely die in the mulcher. From this perspective, mowing with a cutter bar has a less damaging effect, but the vegetation is affected the most, at least in the short term.

5. Conclusion and outlook

This bachelor thesis aimed to investigate the applicability of UAV-based multispectral remote sensing for measuring the impacts of different viticultural management regimes on inter-row cover crops in Rheinhessen.

The results show that the used method is suitable to detect spectral differences between the differently managed inter-rows and thus to gain information about the influence of the management in the inter rows. Using the multispectral camera, the quadrocopter, and the open-source software, accurate and high-resolution orthophotos were obtained, that reached a spatial resolution of about 4 cm and provided a sound basis for further NDVI analyses of the cover crops using GIS.

After the implementation of the inter-row management, all three vineyards showed a statistically significant decrease in NDVI values and thus a reduction in the plant health of the cover crops. However, the extent of this reduction varied between the three areas, probably due to site-specific differences in the environmental background and the management history of the three model vineyards.

Furthermore, it was shown that rolling has the lowest negative impact on the cover crops among the three management regimes studied, thus confirming statements from existing literature. Potentially, this management method can hence be beneficial for various ES, as it protects against erosion and evaporation. Biodiversity also benefits if cover crops are rolled, as flower-rich material becomes available more quickly after implementation. Mowing, on the other hand, causes the greatest disturbance to the vegetation, at least in the short term. This effect could also be confirmed in a spatial dimension in all of the three investigated vineyards.

Representing a new methodological approach, this work lays an important foundation for further research in this area. In addition, it provides methodological support for the *AmBiTo* project, as a part of the ecological research. The standardization of the methodology ensures that the same analysis can be repeated in the following years in the three vineyards or extended to further areas to analyse and document the long-term vegetation changes and occurring patterns in the differently managed vineyards.

Due to the characteristics of the NDVI, the findings do not allow any direct conclusions to be drawn about the long-term vegetation composition or the long-term impacts on biodiversity on the vineyard and landscape level. In this context, in-situ vegetation surveys of all ten model vineyards will provide the first biodiversity-related data in summer of 2022. These data could, in combination with a monitoring of vegetation changes based on UAV remote sensing, provide substantial information about the impacts of different management regimes on biodiversity.

6. Bibliography

- ABAD, J., HERMOSO DE MENDOZA, I., MARÍN, D., ORCARAY, L. u. L. G. SANTESTEBAN (2021): Cover crops in viticulture. A systematic review (1): Implications on soil characteristics and biodiversity in vineyard. In: *OENO One* 55 (1), S. 295–312. DOI: 10.20870/oeno-one.2021.55.1.3599.
- ABOUTALEBI, M., TORRES-RUA, A. F., MCKEE, M., KUSTAS, W., NIETO, H. u. C. COOPMANS (2018): Behavior of vegetation/soil indices in shaded and sunlit pixels and evaluation of different shadow compensation methods using UAV high-resolution imagery over vineyards. In: *Proceedings of SPIE--the International Society for Optical Engineering* 10664. DOI: 10.1117/12.2305883.
- ALBETIS, J., DUTHOIT, S., GUTTLER, F., JACQUIN, A., GOULARD, M. u. H. POILVÉ, et al. (2017): Detection of Flavescence dorée Grapevine Disease Using Unmanned Aerial Vehicle (UAV) Multispectral Imagery. In: *Remote Sensing* 9 (4), S. 308. DOI: 10.3390/rs9040308.
- BALUJA, J., DIAGO, M. P., BALDA, P., ZORER, R., MEGGIO, F., MORALES, F. u. J. TARDAGUILA (2012): Assessment of vineyard water status variability by thermal and multispectral imagery using an unmanned aerial vehicle (UAV). In: *Irrig Sci* 30 (6), S. 511–522. DOI: 10.1007/s00271-012-0382-9.
- BLANCO-PÉREZ, R., SÁENZ-ROMO, M. G., VICENTE-DÍEZ, I., IBÁÑEZ-PASCUAL, S., MARTÍNEZ-VILLAR, E. u. V. S. MARCO-MANCEBÓN, et al. (2020): Impact of vineyard ground cover management on the occurrence and activity of entomopathogenic nematodes and associated soil organisms. In: *Agriculture, Ecosystems & Environment* 301, S. 107028. DOI: 10.1016/j.agee.2020.107028.
- BOLLAS, N., KOKINO, E. u. V. POLYCHRONOS (2021): Comparison of Sentinel-2 and UAV Multispectral Data for Use in Precision Agriculture: An Application from Northern Greece. In: *Drones* 5 (2), S. 35. DOI: 10.3390/drones5020035.
- BOON, M. A., DRIJFHOUT, A. P. u. S. TEFAMICHAEL (2017): Comparison of a fixed-wing and multi-rotor UAV for environmental mapping applications: a case study. In: *Int. Arch. Photogramm. Remote Sens. Spatial Inf. Sci.* XLII-2/W6, S. 47–54. DOI: 10.5194/isprs-archives-XLII-2-W6-47-2017.
- CAMPOS, J., LLOP, J., GALLART, M., GARCÍA-RUIZ, F., GRAS, A., SALCEDO, R. u. E. GIL (2019): Development of canopy vigour maps using UAV for site-specific management during vineyard spraying process. In: *Precision Agric* 20 (6), S. 1136–1156. DOI: 10.1007/s11119-019-09643-z.
- CASTRO, A. I. DE, PEÑA, J. M., TORRES-SÁNCHEZ, J., JIMÉNEZ-BRENES, F. M., VALENCIA-GREDILLA, F., RECASENS, J. u. F. LÓPEZ-GRANADOS (2020): Mapping *Cynodon Dactylon* Infesting Cover Crops with an Automatic Decision Tree-OBIA Procedure and UAV Imagery for Precision Viticulture. In: *Remote Sensing* 12 (1), S. 56. DOI: 10.3390/rs12010056.
- CASTRO, A. I. DE, SHI, Y., MAJA, J. M. u. J. M. PEÑA (2021): UAVs for Vegetation Monitoring: Overview and Recent Scientific Contributions. In: *Remote Sensing* 13 (11), S. 2139. DOI: 10.3390/rs13112139.
- DEUTSCHES WEININSTITUT (Hrsg.) (2022): Deutscher Wein. Statistik '21/'22. Unter Mitarbeit von Eberhard Abele. Online verfügbar unter https://www.deutscheweine.de/fileadmin/user_upload/Website/Service/Downloads/Statistik_2021-2022.pdf, zuletzt geprüft am 21.05.2022.
- EUROPEAN COMMISSION (Hrsg.) (2021): EU biodiversity strategy for 2030. Bringing nature back into our lives.Brussels. Online verfügbar unter <https://data.europa.eu/doi/10.2779/677548>, zuletzt geprüft am 21.05.2022.
- FERRER-GONZÁLEZ, E., AGÜERA-VEGA, F., CARVAJAL-RAMÍREZ, F. u. P. MARTÍNEZ-CARRICONDO (2020): UAV Photogrammetry Accuracy Assessment for Corridor Mapping Based on the Number

- and Distribution of Ground Control Points. In: *Remote Sensing* 12 (15), S. 2447. DOI: 10.3390/rs12152447.
- FRAGA, H., MALHEIRO, A. C., MOUTINHO-PEREIRA, J. u. J. A. SANTOS (2012): An overview of climate change impacts on European viticulture. In: *Food Energy Secur* 1 (2), S. 94–110. DOI: 10.1002/fes3.14.
- FRANZINI, M., RONCHETTI, G., SONA, G. u. V. CASELLA (2019): Geometric and Radiometric Consistency of Parrot Sequoia Multispectral Imagery for Precision Agriculture Applications. In: *Applied Sciences* 9 (24), S. 5314. DOI: 10.3390/app9245314.
- GATTULLO, C. E., MEZZAPESA, G. N., STELLACCI, A. M., FERRARA, G., OCCHIOGROSSO, G. u. G. PETRELLI, et al. (2020): Cover Crop for a Sustainable Viticulture: Effects on Soil Properties and Table Grape Production. In: *Agronomy* 10 (9), S. 1334. DOI: 10.3390/agronomy10091334.
- GEMMICH, A. R. (2017): Blühende Vielfalt im Weinberg (edition graafmann & schreck Wein-Plus Solutions GmbH) Erlangen.
- GILHAUS, K., BOCH, S., FISCHER, M., HÖLZEL, N., KLEINEBECKER, T. u. D. PRATI, et al. (2017): Grassland management in Germany: effects on plant diversity and vegetation composition. In: *Tuexenia* 37, S. 379-397. DOI: 10.14471/2017.37.010.
- GRENDZDÖRFFER (2019): Multispektrale Fernerkundung mit Drohnen. In: *UAV 2019 - Geodäten erobern den Luftraum. Beiträge zum 178. DVW-Seminar am 4. und 5. Februar 2019 in Berlin*. Band 94. ISBN: 978-3-95786-203-7.
- GROOS, A. R., BERTSCHINGER, T. J., KUMMER, C. M., ERLWEIN, S., MUNZ, L. u. A. PHILIPP (2019): The Potential of Low-Cost UAVs and Open-Source Photogrammetry Software for High-Resolution Monitoring of Alpine Glaciers: A Case Study from the Kanderfirn (Swiss Alps). In: *Geosciences* 9 (8), S. 356. DOI: 10.3390/geosciences9080356.
- GUERRA, B. u. K. STEENWERTH (2012): Influence of Floor Management Technique on Grapevine Growth, Disease Pressure, and Juice and Wine Composition: A Review. In: *American Journal of Enology and Viticulture* 63 (2), S. 149–164. DOI: 10.5344/ajev.2011.10001.
- HALL, R. M., PENKE, N., KRIECHBAUM, M., KRATSCHMER, S., JUNG, V. u. S. CHOLLET, et al. (2020): Vegetation management intensity and landscape diversity alter plant species richness, functional traits and community composition across European vineyards. In: *Agricultural Systems* 177, S. 102706. DOI: 10.1016/j.agsy.2019.102706.
- HAN, L., YANG, G., DAI, H., XU, B., YANG, H. u. H. FENG, et al. (2019): Modeling maize above-ground biomass based on machine learning approaches using UAV remote-sensing data. In: *Plant methods* 15, S. 10. DOI: 10.1186/s13007-019-0394-z.
- HANNAH, L., ROEHRDANZ, P. R., IKEGAMI, M., SHEPARD, A. V., SHAW, M. R. u. G. TABOR, et al. (2013): Climate change, wine, and conservation. In: *Proceedings of the National Academy of Sciences of the United States of America* 110 (17), S. 6907–6912. DOI: 10.1073/pnas.1210127110.
- HECKER, L. P., WÄTZOLD, F., YANG, X. u. K. BIRKHOFFER (2022): Squeeze it or leave it? An ecological-economic assessment of the impact of mower conditioners on arthropod populations in grassland. In: *J Insect Conserv.* DOI: 10.1007/s10841-022-00392-5.
- HOFMANN, U. (Hrsg.) (2014): Biologischer Weinbau. (Ulmer) Stuttgart.
- HOLMAN, F. H., RICHE, A. B., CASTLE, M., WOOSTER, M. J. u. M. J. HAWKESFORD (2019): Radiometric Calibration of ‘Commercial off the Shelf’ Cameras for UAV-Based High-Resolution Temporal Crop Phenotyping of Reflectance and NDVI. In: *Remote Sensing* 11 (14), S. 1657. DOI: 10.3390/rs11141657.

- HUANG, S., TANG, L., HUPY, J. P., WANG, Y. u. G. SHAO (2021): A commentary review on the use of normalized difference vegetation index (NDVI) in the era of popular remote sensing. In: *J. For. Res.* 32 (1), S. 1–6. DOI: 10.1007/s11676-020-01155-1.
- INTERGOVERNMENTAL PANEL ON CLIMATE CHANGE (Hrsg.) (2018): Global Warming of 1.5 °C. An IPCC Special Report on the impacts of global warming of 1.5°C above pre-industrial levels and related global greenhouse gas emission pathways, in the context of strengthening the global response to the threat of climate change, sustainable development, and efforts to eradicate poverty. IPCC. Genf.
- JIMÉNEZ-JIMÉNEZ, S. I., OJEDA-BUSTAMANTE, W., MARCIAL-PABLO, M. u. J. ENCISO (2021): Digital Terrain Models Generated with Low-Cost UAV Photogrammetry: Methodology and Accuracy. In: *IJGI* 10 (5), S. 285. DOI: 10.3390/ijgi10050285.
- KATAYAMA, N., BOUAM, I., KOSHIDA, C. u. Y. G. BABA (2019): Biodiversity and yield under different land-use types in orchard/vineyard landscapes: A meta-analysis. In: *Biological Conservation* 229, S. 125–133. DOI: 10.1016/j.biocon.2018.11.020.
- KHALIQ, A., COMBA, L., BIGLIA, A., RICAUDA AIMONINO, D., CHIABERGE, M. u. P. GAY (2019): Comparison of Satellite and UAV-Based Multispectral Imagery for Vineyard Variability Assessment. In: *Remote Sensing* 11 (4), S. 436. DOI: 10.3390/rs11040436.
- KOPAČKOVÁ-STRNADOVÁ, V., KOUCKÁ, L., JELÉNEK, J., LHOTÁKOVÁ, Z. u. F. OULEHLE (2021): Canopy Top, Height and Photosynthetic Pigment Estimation Using Parrot Sequoia Multispectral Imagery and the Unmanned Aerial Vehicle (UAV). In: *Remote Sensing* 13 (4), S. 705. DOI: 10.3390/rs13040705.
- KRAUS, K. (2004⁷): Photogrammetrie: Geometrische Informationen aus Photographien und Laserscanneraufnahmen. (De Gruyter) Berlin.
- LAZCANO, C., GONZALEZ-MALDONADO, N., YAO, E. H., WONG, C. T., MERRILEES, J. J. u. M. FALCONE, et al. (2022): Sheep grazing as a strategy to manage cover crops in Mediterranean vineyards: Short-term effects on soil C, N and greenhouse gas (N₂O, CH₄, CO₂) emissions. In: *Agriculture, Ecosystems & Environment* 327, S. 107825. DOI: 10.1016/j.agee.2021.107825.
- LIBRÁN-EMBED, F. u. I. GRAß (2020): Unmanned aerial vehicles for biodiversity-friendly agricultural landscapes. A systematic review. In: *The science of the total environment*. DOI: 10.1016/j.scitotenv.2020.139204.
- MATESE, A. u. S. DI GENNARO (2018): Practical Applications of a Multisensor UAV Platform Based on Multispectral, Thermal and RGB High Resolution Images in Precision Viticulture. In: *Agriculture* 8 (7), S. 116. DOI: 10.3390/agriculture8070116.
- MATESE, A. u. S. F. DI GENNARO (2021): Beyond the traditional NDVI index as a key factor to mainstream the use of UAV in precision viticulture. In: *Scientific reports* 11 (1), S. 2721. DOI: 10.1038/s41598-021-81652-3.
- MATESE, A., TOSCANO, P., DI GENNARO, S., GENESIO, L., VACCARI, F. u. J. PRIMICERIO, et al. (2015): Intercomparison of UAV, Aircraft and Satellite Remote Sensing Platforms for Precision Viticulture. In: *Remote Sensing* 7 (3), S. 2971–2990. DOI: 10.3390/rs70302971.
- MOLOTOKS, A., KUHNERT, M., DAWSON, T. u. P. SMITH (2017): Global Hotspots of Conflict Risk between Food Security and Biodiversity Conservation. In: *Land* 6 (4), S. 67. DOI: 10.3390/land6040067.
- OLSSON, P.-O., VIVEKAR, A., ADLER, K., GARCIA MILLAN, V. E., KOC, A., ALAMRANI, M. u. L. EKLUNDH (2021): Radiometric Correction of Multispectral UAS Images: Evaluating the Accuracy of the Parrot Sequoia Camera and Sunshine Sensor. In: *Remote Sensing* 13 (4), S. 577. DOI: 10.3390/rs13040577.

- PAIOLA, A., ASSANDRI, G., BRAMBILLA, M., ZOTTINI, M., PEDRINI, P. u. J. NASCIMBENE (2020): Exploring the potential of vineyards for biodiversity conservation and delivery of biodiversity-mediated ecosystem services: A global-scale systematic review. In: *The science of the total environment* 706, S. 135839. DOI: 10.1016/j.scitotenv.2019.135839.
- PELL, T., LI, J. Y. Q. u. K. E. JOYCE (2022): Demystifying the Differences between Structure-from-Motion Software Packages for Pre-Processing Drone Data. In: *Drones* 6 (1), S. 24. DOI: 10.3390/drones6010024.
- PERSSON, M., LINDBERG, E. u. H. REESE (2018): Tree Species Classification with Multi-Temporal Sentinel-2 Data. In: *Remote Sensing* 10 (11), S. 1794. DOI: 10.3390/rs10111794.
- PREUB, J. (2003): Natürliche Rahmenbedingungen Rheinhessens. Heide, Birgit (Hrsg.). Leben und Sterben in der Steinzeit. Ausstellung im Landesmuseum Mainz, 22. Juni - 21. September 2003. Mainz: von Zabern. S. 2-16.
- PROSDOCIMI, M., CERDÀ, A. u. P. TAROLLI (2016): Soil water erosion on Mediterranean vineyards: A review. In: *CATENA* 141, S. 1–21. DOI: 10.1016/j.catena.2016.02.010.
- PUIG-MONTSERRAT, X., STEFANESCU, C., TORRE, I., PALET, J., FÀBREGAS, E. u. J. DANTART, et al. (2017): Effects of organic and conventional crop management on vineyard biodiversity. In: *Agriculture, Ecosystems & Environment* 243, S. 19–26. DOI: 10.1016/j.agee.2017.04.005.
- PUNNAT CHANGSALAK u. PIMONRAT TIANSAWAT (2022): Comparison of Seedling Detection and Height Measurement Using 3D Point Cloud Models from Three Software Tools: Applications in Forest Restoration. In: *EnvironmentAsia* 15, Special, S. 100-105. DOI: 10.14456/ea.2022.26.
- RYSIK, A., CHABUZ, W., SAWICKA-ZUGAJ, W., ZDULSKI, J., GRZYWACZEWSKI, G. u. M. KULIK (2021): Comparative impacts of grazing and mowing on the floristics of grasslands in the buffer zone of Polesie National Park, eastern Poland. In: *Global Ecology and Conservation* 27, e01612. DOI: 10.1016/j.gecco.2021.e01612.
- SCHMIDT, A., KIRMER, A., KIEHL, K. u. S. TISCHEW (2020): Seed mixture strongly affects species-richness and quality of perennial flower strips on fertile soil. In: *Basic and applied ecology*. DOI: 10.1016/j.baae.2019.11.005.
- SHEN, M., CHEN, J., ZHU, X. u. Y. TANG (2009): Yellow flowers can decrease NDVI and EVI values: evidence from a field experiment in an alpine meadow. In: *Canadian Journal of Remote Sensing* 35 (2), S. 99–106. DOI: 10.5589/m09-003.
- SHEN, M., CHEN, J., ZHU, X., TANG, Y. u. X. CHEN (2010): Do flowers affect biomass estimate accuracy from NDVI and EVI? In: *International Journal of Remote Sensing* 31 (8), S. 2139–2149. DOI: 10.1080/01431160903578812.
- STEINGÖTTER, K. (2005): Geologie von Rheinland-Pfalz. (Schweizerbart) Stuttgart.
- TÓTH, V. R. (2018): Monitoring Spatial Variability and Temporal Dynamics of Phragmites Using Unmanned Aerial Vehicles. In: *Frontiers in plant science* 9, S. 728. DOI: 10.3389/fpls.2018.00728.
- VACCA, G. (2019): OVERVIEW OF OPEN SOURCE SOFTWARE FOR CLOSE RANGE PHOTOGRAMMETRY. In: *Int. Arch. Photogramm. Remote Sens. Spatial Inf. Sci.* XLII-4/W14, S. 239–245. DOI: 10.5194/isprs-archives-XLII-4-W14-239-2019.
- VELLEMU, E. C., KATONDA, V., YAPUWA, H., MSUKU, G., NKHOMA, S. u. C. MAKWAKWA, et al. (2021): Using the Mavic 2 Pro drone for basic water quality assessment. In: *Scientific African* 14, e00979. DOI: 10.1016/j.sciaf.2021.e00979.
- VILLOSLADA PECIÑA, M., BERGAMO, T. F., WARD, R. D., JOYCE, C. B. u. K. SEPP (2021): A novel UAV-based approach for biomass prediction and grassland structure assessment in coastal meadows. In: *Ecological Indicators* 122, S. 107227. DOI: 10.1016/j.ecolind.2020.107227.

- WACHENDORF, M., FRICKE, T. u. T. MÖCKEL (2018): Remote sensing as a tool to assess botanical composition, structure, quantity and quality of temperate grasslands. In: *Grass Forage Sci* 73 (1), S. 1–14. DOI: 10.1111/gfs.12312.
- WILSON, H., WONG, J. S., THORP, R. W., MILES, A. F., DAANE, K. M. u. M. A. ALTIERI (2018): Summer Flowering Cover Crops Support Wild Bees in Vineyards. In: *Environmental entomology* 47 (1), S. 63–69. DOI: 10.1093/ee/nvx197.
- WINTER, S., BAUER, T., STRAUSS, P., KRATSCHMER, S., PAREDES, D. u. D. POPESCU, et al. (2018): Effects of vegetation management intensity on biodiversity and ecosystem services in vineyards: A meta-analysis. In: *The Journal of applied ecology* 55 (5), S. 2484–2495. DOI: 10.1111/1365-2664.13124.
- YA'ACOB, N., AZIZE, A. B. M., MAHMON, N. A., YUSOF, A. L., AZMI, N. F. u. N. MUSTAFA (2014): Temporal Forest Change Detection and Forest Health Assessment using Remote Sensing. In: *IOP Conf. Ser.: Earth Environ. Sci.* 19, S. 12017. DOI: 10.1088/1755-1315/19/1/012017.
- ZANETTIN, G., BULLO, A., POZZEBON, A., BURGIO, G. u. C. DUSO (2021): Influence of Vineyard Inter-Row Groundcover Vegetation Management on Arthropod Assemblages in the Vineyards of North-Eastern Italy. In: *Insects* 12 (4). DOI: 10.3390/insects12040349.
- ZIMMERMAN, T., JANSEN, K. u. J. MILLER (2020): Analysis of UAS Flight Altitude and Ground Control Point Parameters on DEM Accuracy along a Complex, Developed Coastline. In: *Remote Sensing* 12 (14), S. 2305. DOI: 10.3390/rs12142305.

7. Appendices

List of appendices

Appendix 1:	Example pictures of the inter-rows before the inter-row management	39
Appendix 2:	Example pictures after the inter-row management.....	42
Appendix 3:	Digital surface models of a) A1, b) A2, and c) A3	44
Appendix 4:	Experimental designs of a) A2 and b) A3.	46
Appendix 5:	Flight routes of the DJI quadrocopter on a) A1, b) A2, and c) A3.....	47
Appendix 6:	NDVI images of the model vineyards.....	49
Appendix 7:	Dot chart and histogram of the whole data set to test visually for normal distribution of the residuals	52
Appendix 8:	R scripts used in the bachelor thesis.....	53
Appendix 9:	Example of the buffers (a) and random point samples (b) generated on A3	56
Appendix 10:	Additional results of the conducted covariance analysis.....	57

Appendix 1: Example pictures of the inter-rows before the inter-row management
(Source: own recordings).



A2, inter-row 18 (rolling)



A2, inter-row 22 (mowing)



A2, inter-row 20 (mulching)



A3, inter-row 10 (rolling)



A3, inter-row 12 (mulching)



A3, inter-row 8 (mulching)



Appendix 2: Example pictures after the inter-row management (Source: own recordings).

A2, inter-row 18 (rolling)



A2, inter-row 22 (mowing)

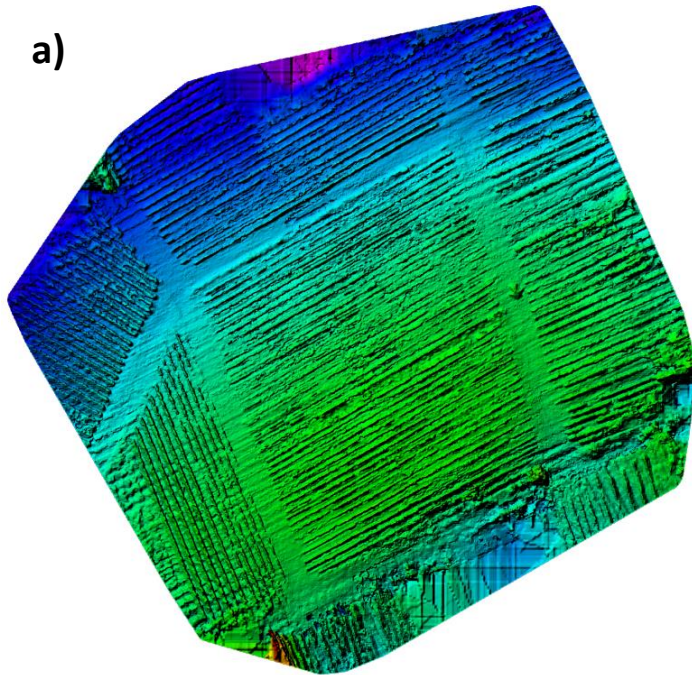


A2, inter-row 20 (mulching)

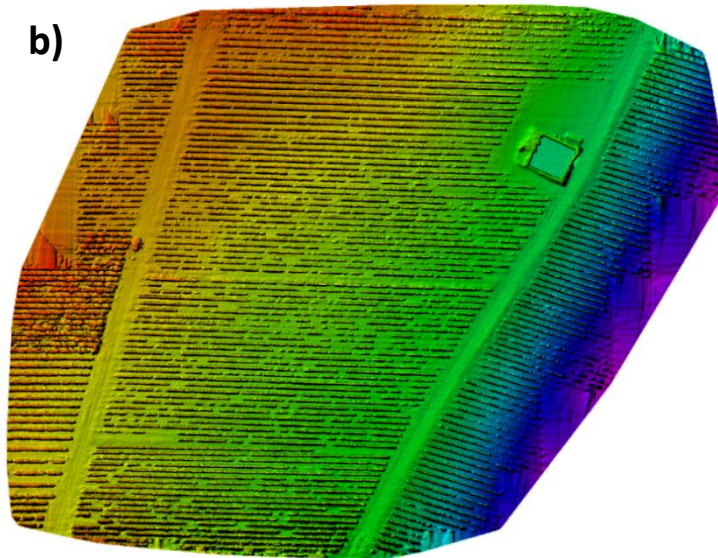


Appendix 3: Digital surface models of a) A1, b) A2, and c) A3 (source: own representation).

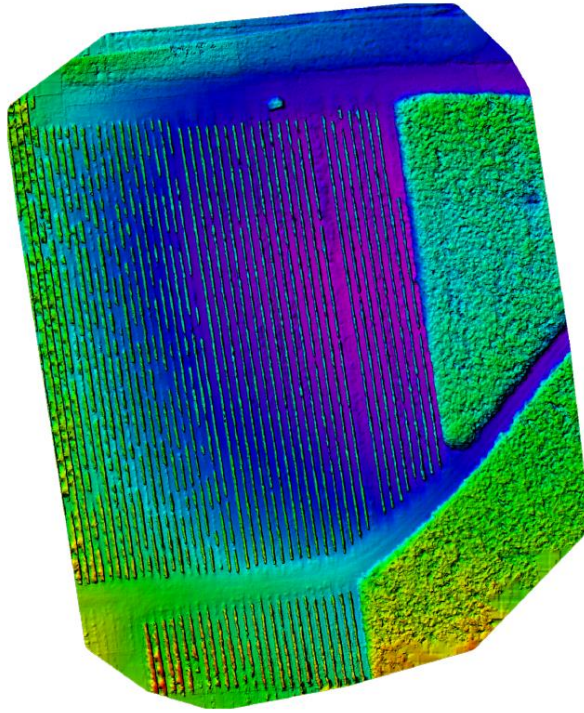
a)



b)



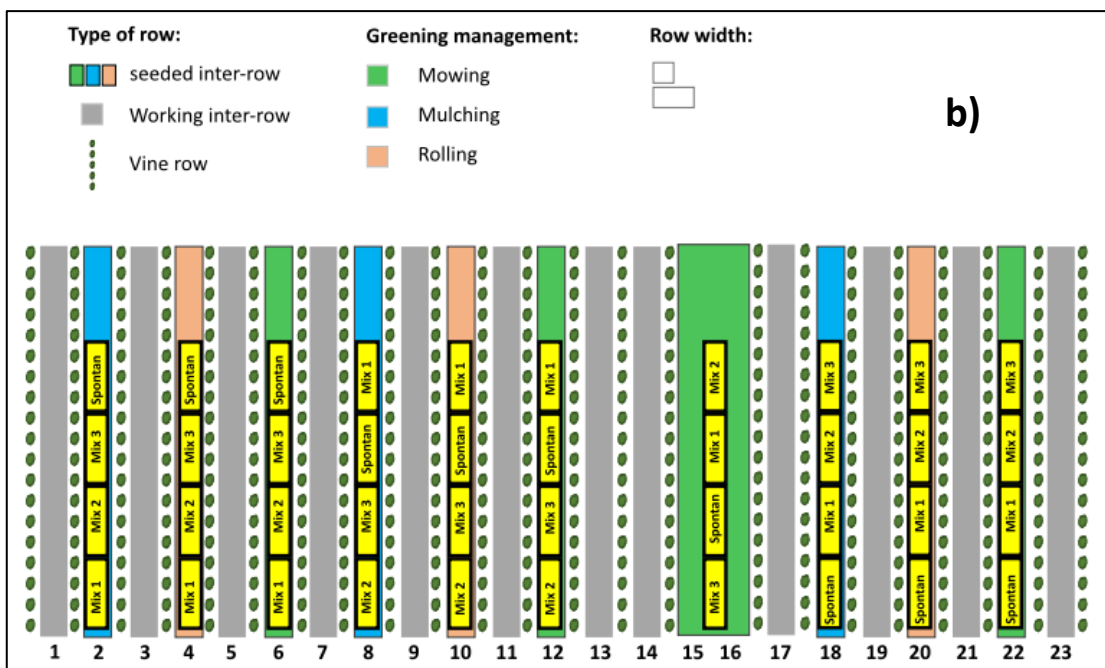
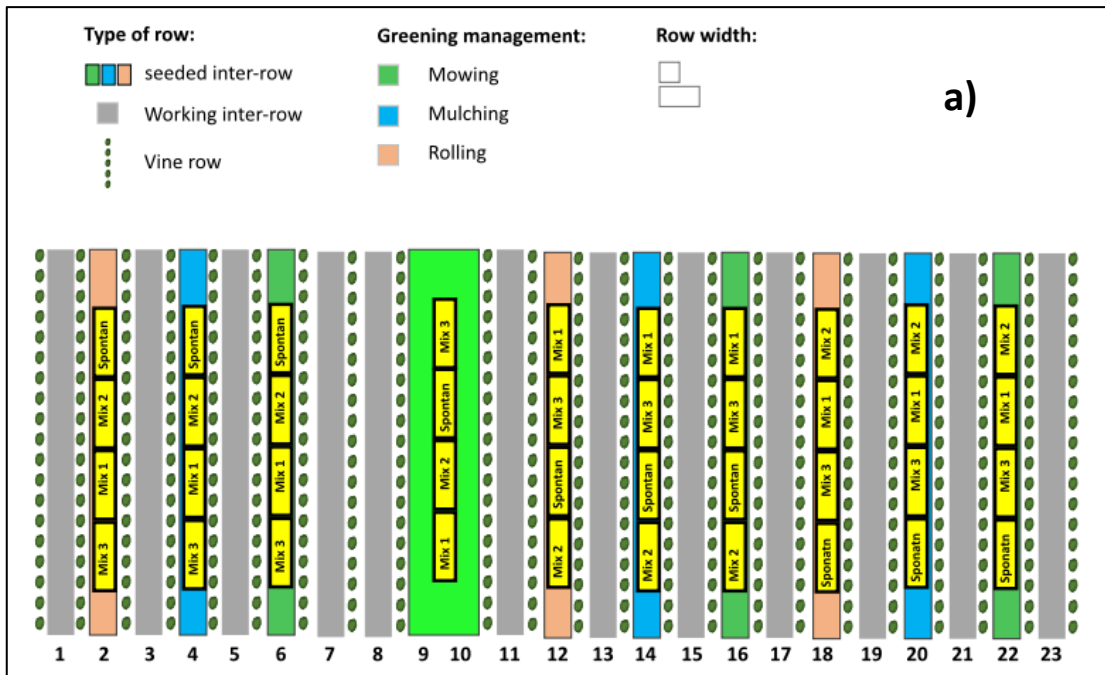
c)



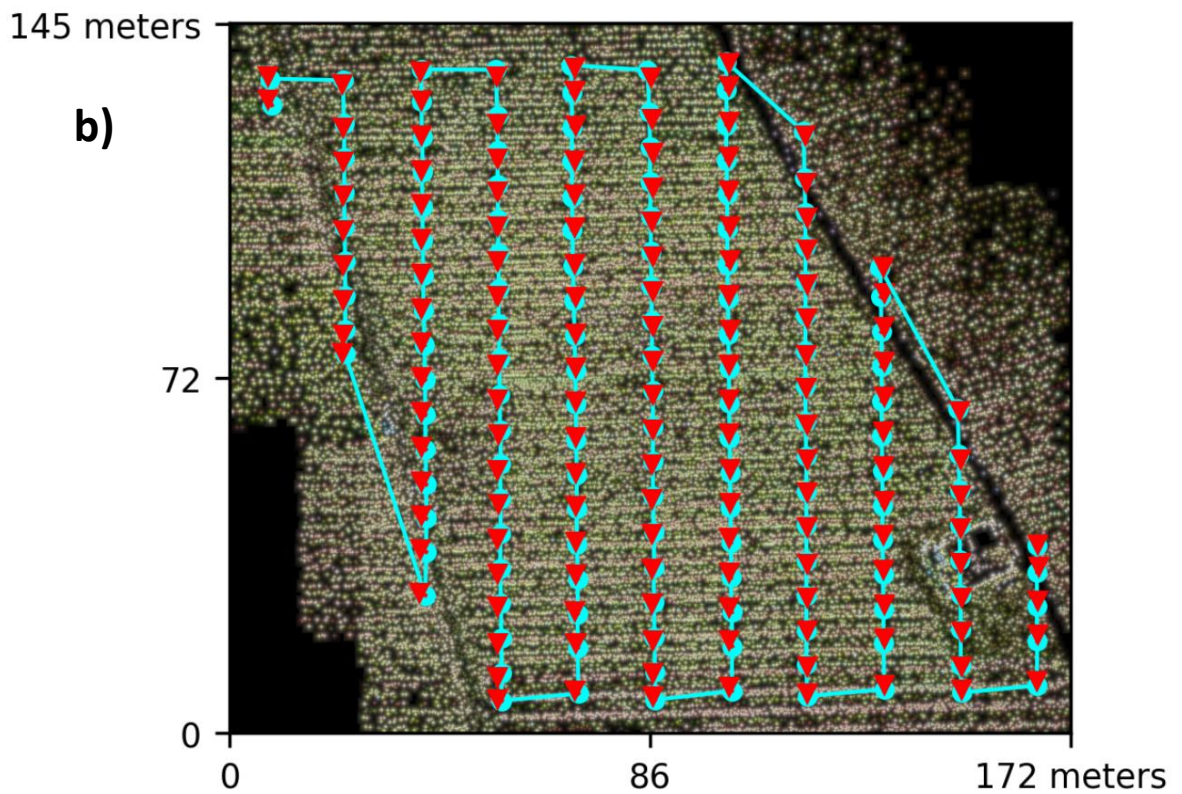
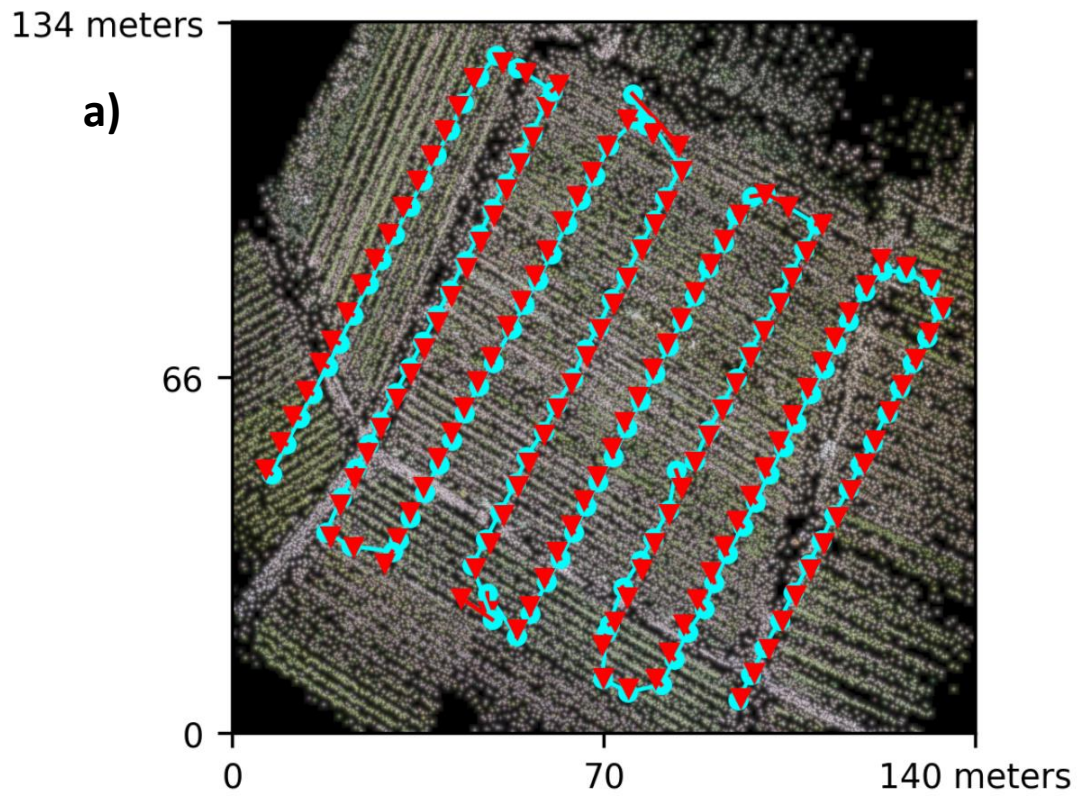
Digital Surface Model

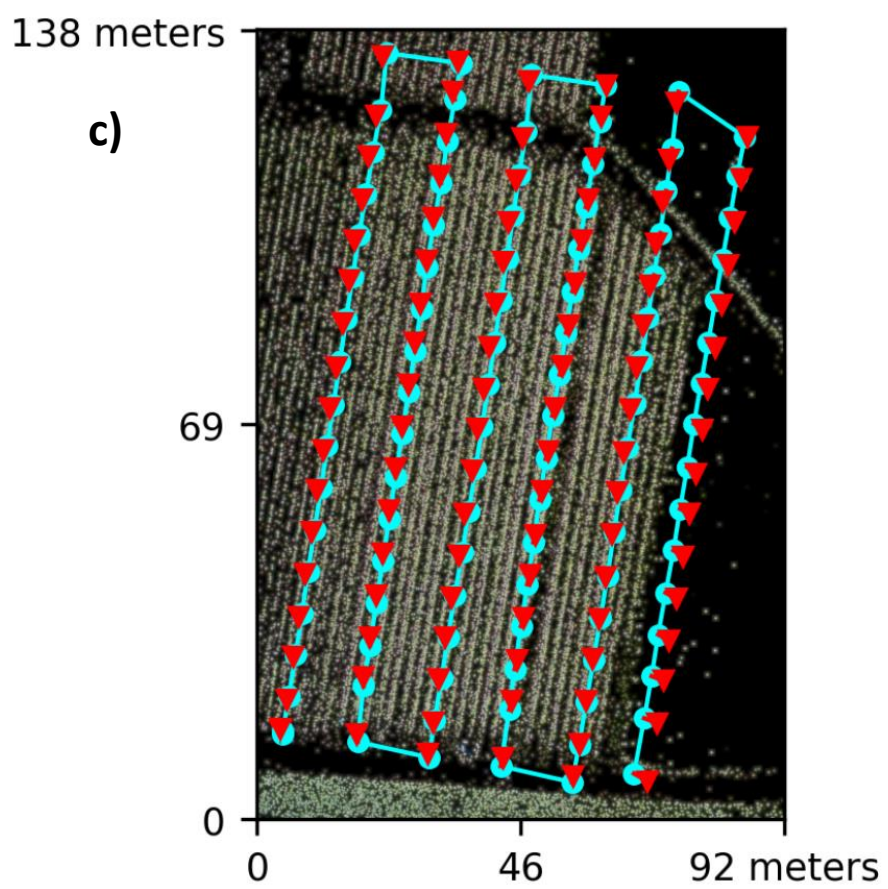


Appendix 4: Experimental designs of a) A2 and b) A3 (Source: own representation based on the AmBiTo project).

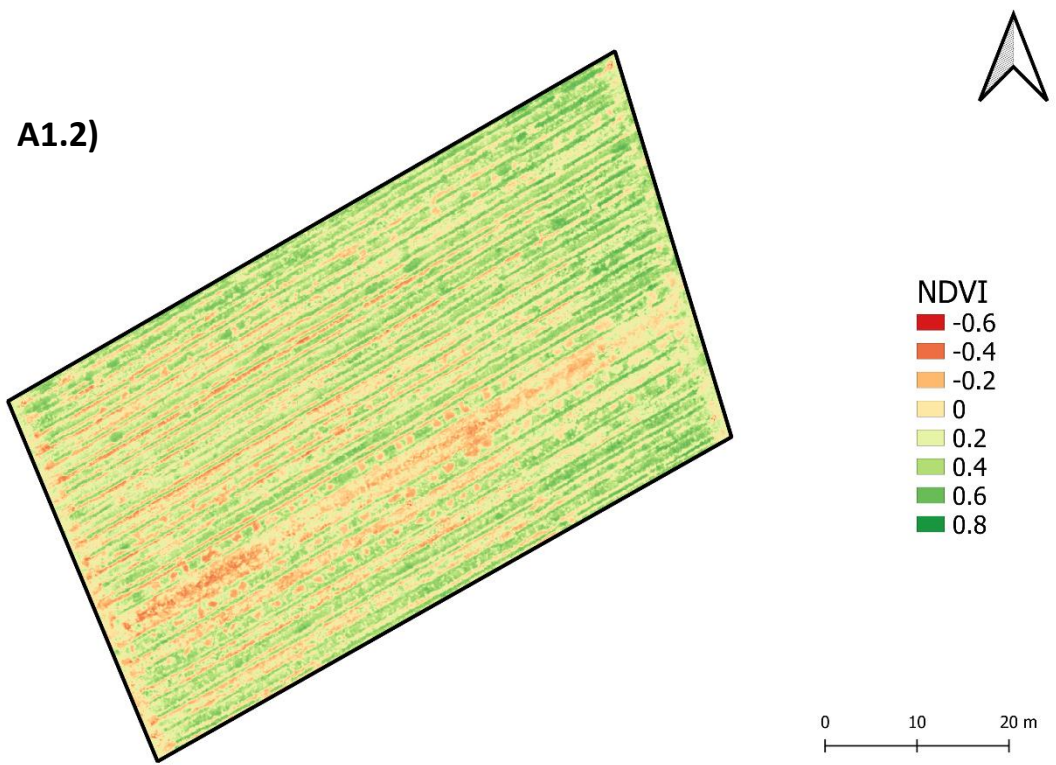
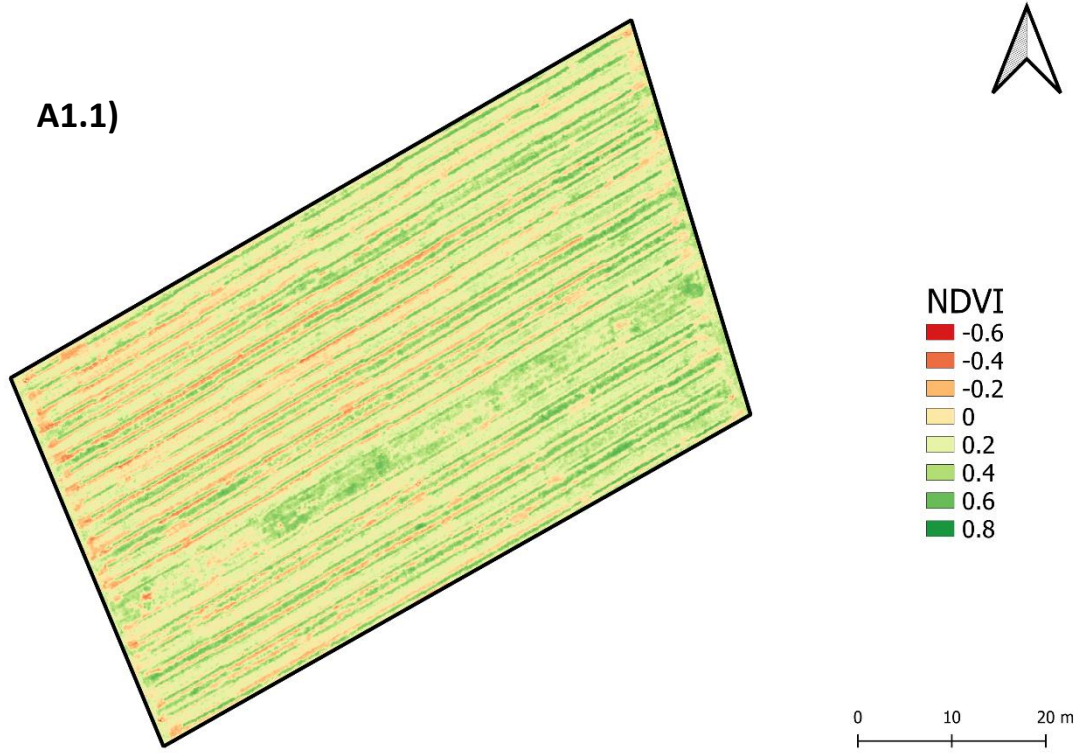


Appendix 5: Flight routes of the DJI quadcopter on a) A1, b) A2, and c) A3. The red triangles represent the orientation of the Mavic 2 Pro, and the blue dots represent the single images taken by the Hasselblad camera of the Mavic 2 Pro. (source: own representation).

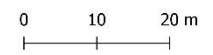
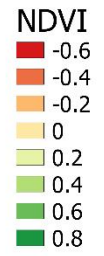
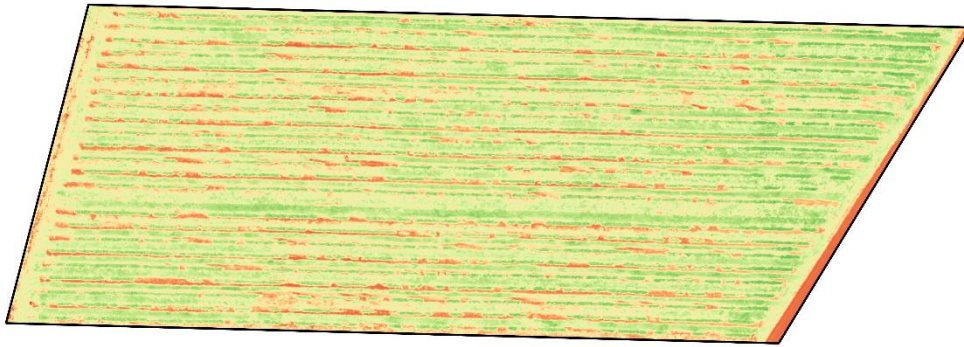




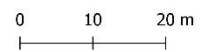
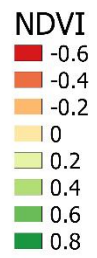
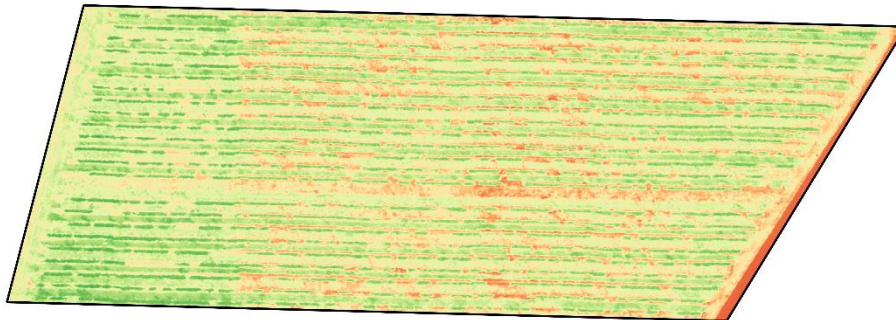
Appendix 6: NDVI images of the model vineyards.



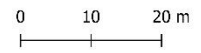
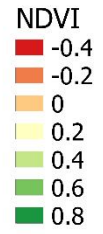
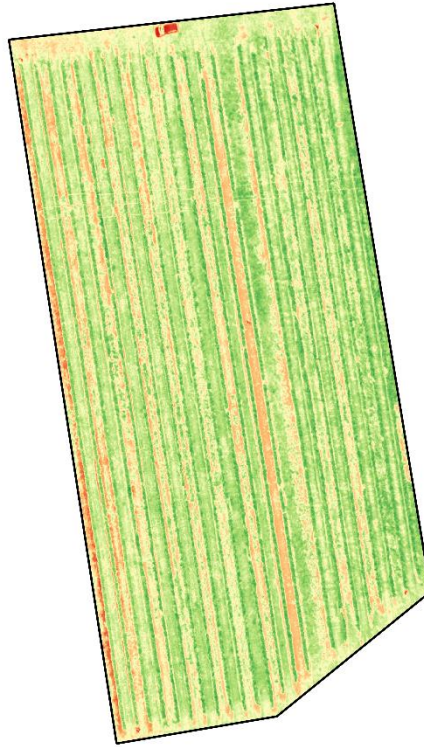
A2.1)



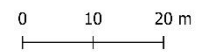
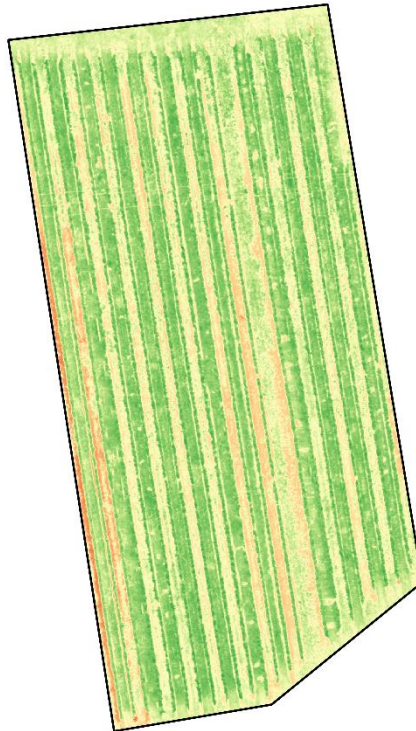
A2.2)



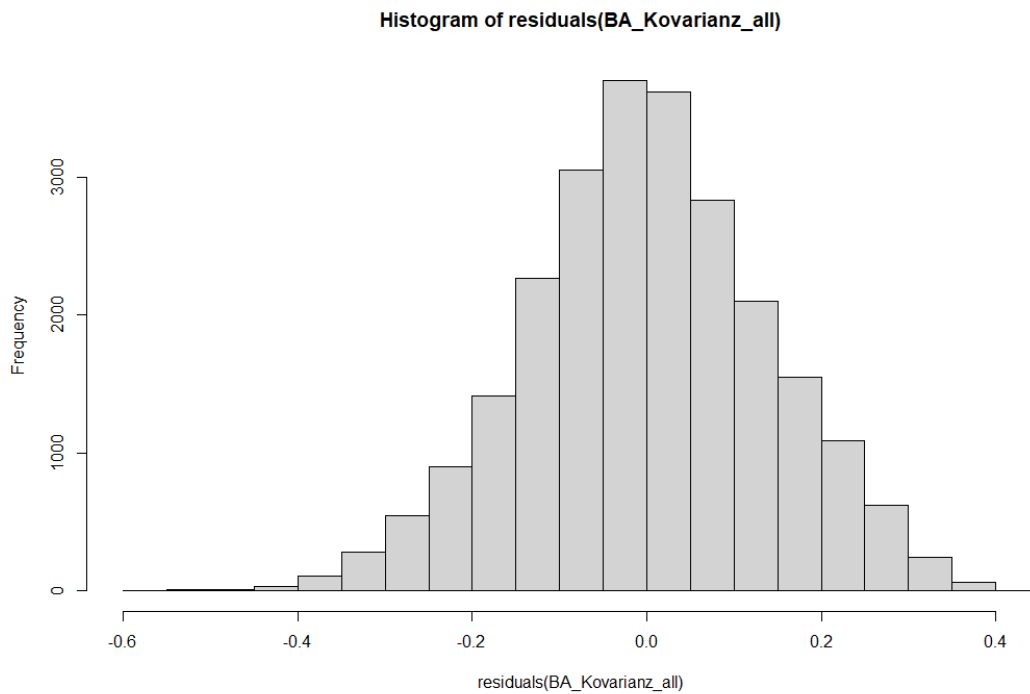
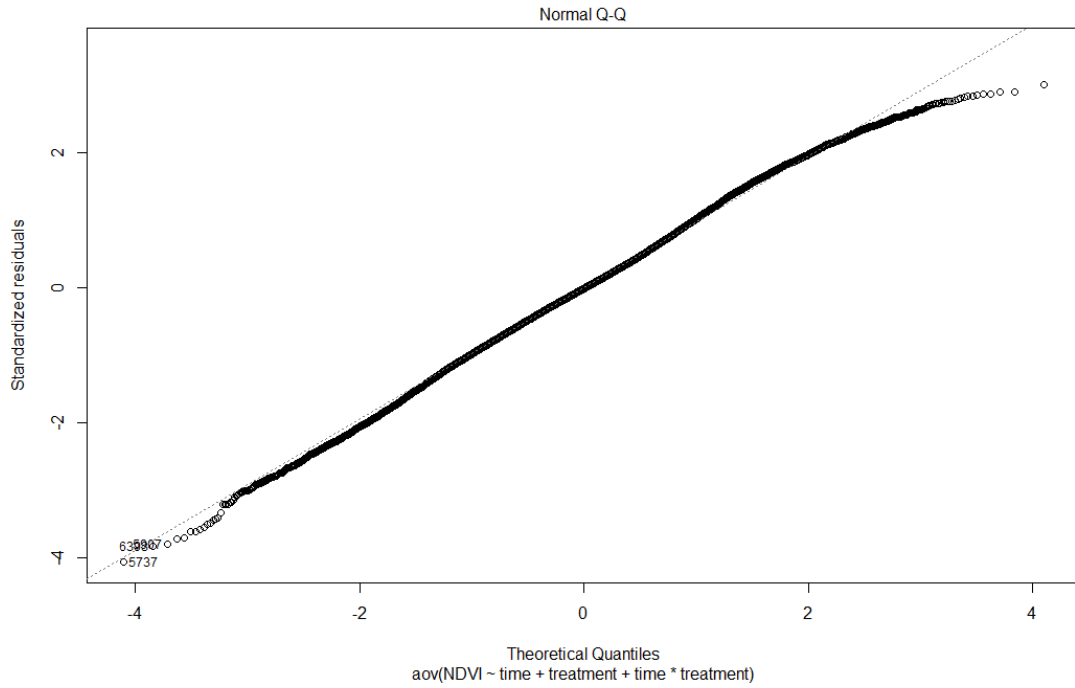
A3.1)



A3.2)



Appendix 7: Dot chart and histogram of the whole data set to test visually for normal distribution of the residuals. The test is a prerequisite for conducting a two-factor covariance analysis (Source: own representation).



Appendix 8: R scripts used in the bachelor thesis.

```
##### Bachelor Thesis #####
```

#PREPARATION

```
#import data set
```

```
library(readxl)
```

```
BA_datensatz <- read_excel("C:/Users/noahg/OneDrive/Bachelorarbeit/Excel-  
Dokumente/BA_point_sample_all_untereinander_alpha.xlsx")
```

```
#create subsets
```

```
BA_datensatz_area1 <- subset(BA_datensatz, area==1)
```

```
BA_datensatz_area2 <- subset(BA_datensatz, area==2)
```

```
BA_datensatz_area3 <- subset(BA_datensatz, area==3)
```

#DESCRIPTIVE STATISTICS

```
library(psych)
```

```
describeBy(NDVI ~ treatment + time, data=BA_datensatz)
```

```
describeBy(NDVI ~ treatment + time, data=BA_datensatz_area1)
```

```
describeBy(NDVI ~ treatment + time, data=BA_datensatz_area2)
```

```
describeBy(NDVI ~ treatment + time, data=BA_datensatz_area3)
```

#COVARIANCE ANALYSIS

```
#Visual checking the normal distribution residuals using QQ-plots and histograms
```

```
plot(BA_Kovarianz_all, 2)
```

```
plot(BA_Kovarianz_area1, 2)
```

```
plot(BA_Kovarianz_area2, 2)
```

```
plot(BA_Kovarianz_area3, 2)
```

```
hist(residuals(BA_Kovarianz_all))
```

```
hist(residuals(BA_Kovarianz_area1))
```

```
hist(residuals(BA_Kovarianz_area2))
```

```
hist(residuals(BA_Kovarianz_area3))
```

```

#Covariance analysis for the whole data set

BA_Kovarianz_all <- lm(NDVI ~ time + treatment + time*treatment, data = BA_datensatz)

summary(BA_Kovarianz_all)

anova(BA_Kovarianz_all)

#Covariance analysis for area 1

BA_Kovarianz_area1 <- lm(NDVI ~ time + treatment + time*treatment, data = BA_datensatz_area1)

summary(BA_Kovarianz_area1)

anova(BA_Kovarianz_area1)

# Covariance analysis for area 2

BA_Kovarianz_area2 <- lm(NDVI ~ time + treatment + time*treatment, data = BA_datensatz_area2)

summary(BA_Kovarianz_area2)

anova(BA_Kovarianz_area2)

# Covariance analysis for area3

BA_Kovarianz_area3 <- lm(NDVI ~ time + treatment + time*treatment, data = BA_datensatz_area3)

summary(BA_Kovarianz_area3)

anova(BA_Kovarianz_area3)

#FIGURES

#Boxplots for management and time

boxplot(NDVI ~ time + treatment, data = BA_datensatz,

        main = "NDVI values by time and management",

        xlab = "Management and time",

        ylab = "NDVI",

        ylim = c(-0.4, 0.8),

        col = (c("steelblue", "lightblue", "steelblue", "lightblue", "steelblue", "lightblue"),

        border = "black"))

boxplot(NDVI ~ time + treatment, data = BA_datensatz_area1,

        main = "NDVI values by time and management",

        xlab = "Time and management",

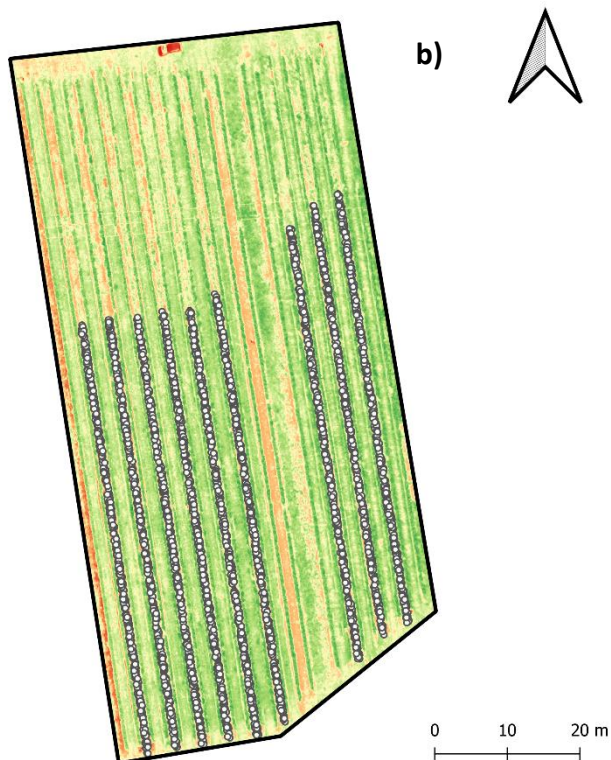
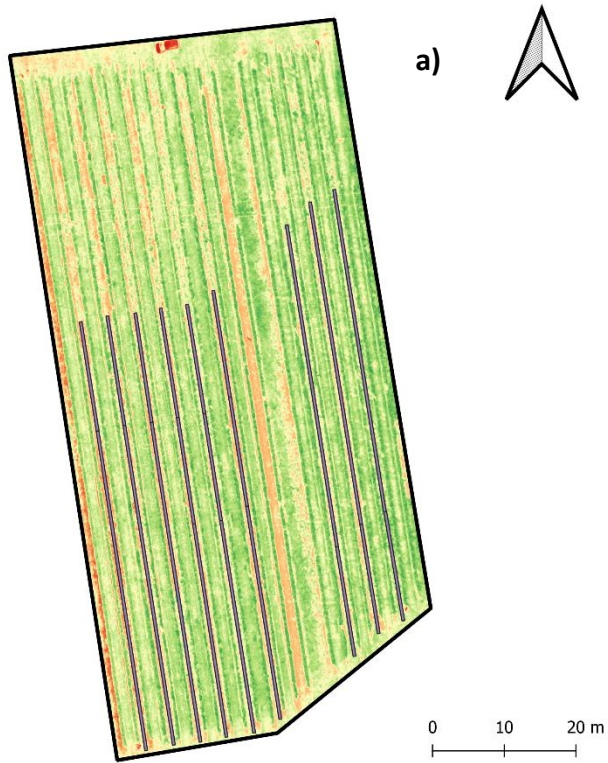
```

```
ylab = "NDVI",  
ylim = c(-0.4, 0.8),  
col = (c("steelblue", "lightblue", "steelblue", "lightblue", "steelblue", "lightblue",  
border = "black"))))
```

```
boxplot(NDVI ~ time + treatment, data = BA_datensatz_area2,  
main = "NDVI values by time and management",  
xlab = "Time and management",  
ylab = "NDVI",  
ylim = c(-0.4, 0.8),  
col = (c("steelblue", "lightblue", "steelblue", "lightblue", "steelblue", "lightblue",  
border = "black"))))
```

```
boxplot(NDVI ~ time + treatment, data = BA_datensatz_area3,  
main = "NDVI values by time and management",  
xlab = "Time and management",  
ylab = "NDVI",  
ylim = c(-0.4, 0.8),  
col = (c("steelblue", "lightblue", "steelblue", "lightblue", "steelblue", "lightblue",  
border = "black"))))
```

Appendix 9: Example of the buffers (a) and random point samples (b) generated on A3 (NDVI image before the inter-row management) in order to extract the NDVI values (Source: own representation).



Appendix 10: Additional results of the conducted covariance analysis (Source: own representation).

		Df	Sum of squares	Root mean square (RMS)	F-value	p-value
A1	Time	1	80.89	80.89	4356.13	<0.001
	Management regime	2	14.07	7.04	378.88	<0.001
	Time*Managment regime	2	6.22	3.10	167.44	<0.001
A2	Time	1	9.85	9.85	953.69	<0.001
	Management regime	2	8.24	4.12	398.83	<0.001
	Time*Managment regime	2	2.47	1.24	119.61	<0.001
A3	Time	1	0.27	0.27	19.94	<0.001
	Management regime	2	2.67	1.33	97.97	<0.001
	Time*Managment regime	2	2.02	1.0	74.17	<0.001

